



HAL
open science

Essential role of the plant DNA polymerase theta for the repair of replication-associated DNA damage under standard and abiotic stress conditions

Maherun Nisa, Clara Bergis, Jose-Antonio Pedroza-Garcia, Jeannine Drouin-Wahbi, Christelle Mazubert, Catherine Bergounioux, Moussa Benhamed, Cécile Raynaud

► To cite this version:

Maherun Nisa, Clara Bergis, Jose-Antonio Pedroza-Garcia, Jeannine Drouin-Wahbi, Christelle Mazubert, et al.. Essential role of the plant DNA polymerase theta for the repair of replication-associated DNA damage under standard and abiotic stress conditions. *The Plant Journal*, 2021, pp.1-40. 10.1111/tpj.15295 . hal-03240087

HAL Id: hal-03240087

<https://hal.science/hal-03240087v1>

Submitted on 27 May 2021

HAL is a multi-disciplinary open access archive for the deposit and dissemination of scientific research documents, whether they are published or not. The documents may come from teaching and research institutions in France or abroad, or from public or private research centers.

L'archive ouverte pluridisciplinaire **HAL**, est destinée au dépôt et à la diffusion de documents scientifiques de niveau recherche, publiés ou non, émanant des établissements d'enseignement et de recherche français ou étrangers, des laboratoires publics ou privés.



Distributed under a Creative Commons Attribution 4.0 International License

1 **Essential role of the plant DNA polymerase theta for the repair of replication-**
2 **associated DNA damage under standard and abiotic stress conditions**

3 **Maherun Nisa^{1,2}, Clara Bergis^{1,2}, Jose-Antonio Pedroza-Garcia^{1,2}, Jeannine Drouin-Wahbi^{1,2},**
4 **Christelle Mazubert^{1,2}, Catherine Bergounioux^{1,2}, Moussa Benhamed^{1,2} and Cécile Raynaud^{1,2}**

5 **1 Université Paris-Saclay, CNRS, INRAE, Univ Evry, Institute of Plant Sciences Paris-Saclay**
6 **(IPS2), 91405, Orsay, France.**

7 **2 Université de Paris, CNRS, INRAE, Institute of Plant Sciences Paris Saclay (IPS2) 91405 Orsay**

8 **Running head:** Role of DNA Pol θ in the repair of replication associated DNA damage

9 **ABSTRACT**

10 Safeguard of genome integrity is a key process in all living organisms. Due to their sessile lifestyle,
11 plants are particularly exposed to all kinds of stress conditions that could induce DNA damage.
12 However, very few genes involved in the maintenance of genome integrity are indispensable to
13 plants' viability. One remarkable exception is the *POLQ* gene that encodes DNA polymerase theta
14 (Pol θ), a non-replicative polymerase involved in Trans-Lesion Synthesis (TLS) during DNA
15 replication and Double-Strand Breaks (DSB) repair. The *Arabidopsis* *tebichi* (*teb*) mutants,
16 deficient for Pol θ , have been reported to display severe developmental defects, leading to the
17 conclusion that Pol θ is required for normal plant development. However, this essential role of Pol
18 θ in plants is challenged by contradictory reports regarding the phenotypic defects of *teb* mutants,
19 and the recent finding that rice null mutants develop normally. Here we show that the phenotype
20 of *teb* mutants is highly variable. Taking advantage of hypomorphic mutants for the replicative
21 DNA polymerase ϵ , that display constitutive replicative stress, we show that Pol θ allows
22 maintenance of meristem activity when DNA replication is partially compromised. Furthermore,
23 we found that the phenotype of Pol θ mutants can be aggravated by modifying their growth
24 conditions, suggesting that environmental conditions impact the basal level of replicative stress,
25 and providing evidence for a link between plants' response to adverse conditions, and mechanisms
26 involved in the maintenance of genome integrity.

27 **Key words:** Genome stability, DNA replication, Pol θ , abiotic stress, plants

28 **Significance statement:** Pol θ is one of the few proteins involved in DNA repair that appears to
29 be essential for plant development, but there are contradictory reports concerning the phenotype
30 of Pol θ -deficient mutants. Here we show that Pol θ plays a key role in the repair of replication-
31 associated DNA breaks, and that its requirement for plant development depends on growth
32 conditions, providing evidence for a link between abiotic stress responses and the DNA Damage
33 Response.

34

35 INTRODUCTION

36 Organism's survival depends on the faithful transmission of genetic information. Due to their
37 sessile lifestyle, plants cannot escape stress conditions with the potential to compromise their
38 genome integrity. Indeed, because sunlight is the energy source of plants, they are constantly
39 exposed to UV-radiations, that can cause DNA damage such as pyrimidine dimers. In addition,
40 cellular metabolic activities such as photosynthesis lead to the production of Reactive Oxygen
41 Species (Noctor and Foyer, 2016), that can induce DNA lesions, and whose production can be
42 exacerbated by various biotic and abiotic stress conditions. In plants like in all eukaryotes, DNA
43 lesions are recognized and trigger a signaling cascade called the DNA damage response (DDR)
44 that leads to the activation of cell cycle checkpoints in proliferating cells, and specific DNA repair
45 mechanisms (Ciccia and Elledge, 2010; Yoshiyama *et al.*, 2013; Hu *et al.*, 2016; Nisa *et al.*, 2019).
46 Outcomes of DDR activation may be different depending on the severity of DNA damage and on
47 the efficiency of the repair process: successful repair allows cell survival and resumption of the
48 cell cycle, but if the damage is too severe, it may induce permanent cell proliferation arrest through
49 endoreduplication (Adachi *et al.*, 2011) or even cell death (Fulcher and Sablowski, 2009). The
50 cellular response also depends on the cell type, meristematic cells being more sensitive to DNA
51 damage and more prone to undergo cell death than differentiated cells (Fulcher and Sablowski,
52 2009).

53 Because maintenance of genome integrity relies on its faithful duplication in proliferating cells,
54 and its efficient repair in all cell types, DNA polymerases (Pol) play a pivotal role in this process
55 (Burgers, 1998). In eukaryotes, DNA polymerases are distributed between replicative and non-
56 replicative polymerases (Burgers, 1998), and classified into 4 families (A, B, X and Y), based on
57 the primary structure of their catalytic subunit (Makarova and Koonin, 2013). The three replicative
58 polymerases (DNA Pol α , δ and ϵ) belong to the B-family (Jain *et al.*, 2018) whereas non-
59 replicative polymerases can be found in all families, and are involved in different DNA repair
60 pathways. One distinctive feature of replicative polymerases is their tight catalytic sites that
61 confers them a very low error rate (Kunkel, 2004). Consequently, their progression during DNA
62 replication can be blocked by lesions that are too large to be accommodated in their catalytic site,
63 such as bulky adducts or pyrimidine dimers. When replisome progression is prevented by a DNA
64 lesion on the template strand, non-replicative polymerases that have a looser active site can

65 substitute for canonical replicative ones to perform Trans-Lesion Synthesis (TLS), a process by
66 which they allow the replisome to progress beyond the DNA lesions (Kunkel, 2004; Yang and
67 Gao, 2018). TLS polymerases are thought to associate into a huge complex with stalled replication
68 forks, allowing the choice of the most appropriate one to bypass the lesion, depending on its nature
69 (Powers and Washington, 2018). The high diversity of TLS polymerases likely stems from the fact
70 that they have different so-called cognate lesions, opposite to which they are able to perform error-
71 free DNA synthesis: each TLS polymerase can thus be recruited for efficient error-free bypass of
72 specific lesions (Powers and Washington, 2018). Plant genomes encompass at least 9 non-
73 replicative polymerases, 6 of which have been functionally characterized, and involved in TLS
74 and/or DNA repair: Pol ζ , η , κ , θ , and λ and Reversionless1 (Rev1) (reviewed in (Pedroza-Garcia
75 *et al.*, 2019; Sakamoto, 2019)). Deficiency in non-replicative polymerases usually does not affect
76 overall development, but rather results in hypersensitivity to various DNA-damaging agents
77 (Pedroza-Garcia *et al.*, 2019). One intriguing exception is Pol θ (encoded by the *POLQ* gene) also
78 called TEBICHI in *Arabidopsis thaliana*: *teb* null mutants show severe developmental defects
79 (Inagaki *et al.*, 2006; Inagaki *et al.*, 2009), suggesting that the cellular function of Pol θ is essential
80 for proper development.

81 The knowledge about the molecular function of Pol θ in plants is scarce in comparison to other
82 eukaryotes. In Human cells, Pol θ can perform error-prone TLS through UV-lesions. Its deficiency
83 results in a dramatic increase of tumorigenesis upon UV exposure, indicating that this error-prone
84 TLS is crucial to avoid collapse of stalled forks (Yoon *et al.*, 2019). Another key function of Pol
85 θ is DSB repair through ALternative Non-Homologous End Joining (Alt-NHEJ), also called
86 Micro-homology Mediated End Joining (MMEJ) (Beagan and McVey, 2016). Alt-NHEJ is an
87 error-prone pathway for DSB repair in which resection of DNA ends on each side of the break
88 exposes micro-homology of only a few base pairs, that can allow annealing of single stranded
89 DNA (ssDNA) and subsequent end-joining (Chiruvella *et al.*, 2013). Recently, Mateos-Gomez and
90 colleagues demonstrated that through its helicase domain, Pol θ facilitates the displacement of
91 RPA that normally protects resected ends and promotes homologous recombination (HR), thereby
92 favoring Alt-NHEJ over HR (Mateos-Gomez *et al.*, 2017).

93 This dual role of Pol θ in DSB repair is likely a key factor of the cellular response to replicative
94 (or replication) stress. Replicative stress is a complex phenomenon that arises when fork

95 progression is stopped or slowed-down. If the obstacle cannot be bypassed (for example through
96 TLS), fork stalling triggers the accumulation of single stranded DNA coated by the replication
97 protein RPA, leading to the activation of the ATR (ATM and Rad3-related) kinase and subsequent
98 DDR signaling (reviewed in (Zeman and Cimprich, 2014)). Pol θ is thus assumed both to prevent
99 replicative stress by avoiding fork stalling at DNA lesions, and to contribute to DNA repair when
100 replicative stress results in fork collapse and subsequent DSB formation. Indeed, in Human cells,
101 *POLQ* deficiency confers hypersensitivity to ATR inhibitors, providing evidence for the role of
102 Pol θ for the repair of DNA replication-induced DNA damage (Wang *et al.*, 2019), and a synthetic
103 lethal genetic screen revealed that various components of the DDR are indispensable to cell
104 survival in the absence of Pol θ . The common feature of all mutations identified in the screen was
105 that they caused accumulation of endogenous DNA damage, indicating that the most prominent
106 role of Pol θ is the repair of replication-associated DSB, regardless of the initial cause of DNA
107 damage (Feng *et al.*, 2019). There is thus accumulating evidence that Pol θ is key for repairing
108 DSBs associated with fork collapse due to replication stress, via Alt-NHEJ (Wang *et al.*, 2019;
109 Kelso *et al.*, 2019). Analysis of plant Pol θ mutants suggests that this dual role is conserved in
110 plants. The *teb* mutants show constitutive activation of the DNA Damage Response (DDR),
111 consistent with role of Pol θ in the maintenance of genome integrity (Inagaki *et al.*, 2006). They
112 are more sensitive to UV, and to the DNA alkylating agent methylmethane sulfonate (MMS)
113 (Inagaki *et al.*, 2006), consistent with a TLS function. Furthermore, Pol θ -dependent Alt-NHEJ
114 was identified as the pathway for T-DNA integration after transformation by agrobacterium (van
115 Kregten *et al.*, 2016), although this finding has lately been questioned by the observation that T-
116 DNA integration remains possible, albeit with a reduced efficiency, in Pol θ null mutants
117 (Nishizawa-Yokoi *et al.*, 2020).

118 Two important questions still hold regarding the function of plant Pol θ . First, it is not clear whether
119 the TLS or DSB repair function, or both can account for the fact that this protein is required for
120 normal plant development, as most plant mutants deficient for TLS or DNA repair develop
121 normally in the absence of genotoxic stress. Second, there are conflicting reports regarding the
122 developmental defects caused by Pol θ deficiency, and it thus remains unclear to what extent it is
123 indeed required for normal development. As mentioned above, several *teb* alleles (*teb1*, *teb2* and
124 *teb5*) have been described in Arabidopsis and were all reported to display the same phenotypic

125 alterations including reduced growth, deformed leaves and disorganized root meristems (Inagaki
126 *et al.*, 2006; Inagaki *et al.*, 2009). However, in *Physcomitrella patens*, *polq* mutants were deficient
127 for DSB repair, but did not show any developmental defects (Mara *et al.*, 2019), and authors
128 questioned the requirement of Pol θ for normal development in Arabidopsis, as other groups did
129 not seem to observe severe developmental defects (van Kregten *et al.*, 2016). More recently, *polq*
130 mutants were generated in rice, and reported to develop normally under standard growth
131 conditions, although regeneration from calli was severely impaired (Nishizawa-Yokoi *et al.*,
132 2020).

133 To tackle these questions, we carefully re-examined the phenotype of *teb* mutants, finding that it
134 is highly variable. Furthermore, to try and determine the origin of developmental defects caused
135 by Pol θ deficiency, we took advantage of the *pol2a-4* mutant that is partially deficient in the
136 replicative polymerase Pol ϵ and shows constitutive replicative stress (Pedroza-Garcia *et al.*,
137 2017). Our results indicate that one key cellular function of Pol θ is to avoid DNA damage
138 accumulation during DNA replication, and that developmental defects observed in *teb* mutants are
139 likely consequences of replicative stress. Finally, we show that the phenotype of *teb* mutants can
140 be aggravated by exposure to abiotic stresses, suggesting that environmental conditions impact the
141 basal level of replicative stress, and providing evidence for a link between plant tolerance to stress,
142 and mechanisms involved in the maintenance of genome integrity.

143 **RESULTS**

144 Previous work reported the phenotype of *teb* mutants, with stunted growth and deformed leaves
145 (Inagaki *et al.*, 2006). Five alleles of the mutant were initially described, three of which: *teb1*, *teb2*
146 and *teb5* gave rise to the same phenotype and appeared to be full loss of function mutants (Inagaki
147 *et al.*, 2006) (Figure 1A). However, rice mutants did not show developmental defects (Nishizawa-
148 Yokoi *et al.*, 2020), and other groups reported much milder phenotypical defects for *teb2* and *teb5*
149 mutants (van Kregten *et al.*, 2016). To clarify this, we carefully re-examined the phenotype of
150 these mutants. In our growth conditions, most of the *teb2* and *teb5* mutants appeared
151 indistinguishable from the wild-type after 1 month of growth (Figure 1B). We classified *teb*
152 mutants' phenotypes in two categories: wild type like (WTL) plants appeared identical to the wild-
153 type (Col-0) and plants with severe (S) developmental defects showed the previously described

154 *tebichi* phenotype (Figure 1B). We first checked that both WTL and S plants were homozygous
155 for the *teb* mutation, using primers flanking the T-DNA insertions in *teb2* and *teb5* mutants (Figure
156 1A, C). We also checked by qPCR that both *teb* alleles we used did not allow the expression of
157 the full length *POLQ* mRNA. To this end we used three primer pairs: one (#1) at the 5' end of the
158 *TEB* gene, upstream both insertions, one flanking the T-DNA insertion site of the *teb5* mutant (#2),
159 and one (#3) in the 3' moiety of the gene (Figure 1A). The first primer pair allowed detection of
160 wild-type levels of mRNA in both mutants, indicating that the 5' extremity of the gene is normally
161 expressed (Figure 1D). However, the *teb2* mutant accumulated no detectable transcripts produced
162 downstream of the insertion. Expression of the 3' moiety of the gene was drastically reduced in
163 *teb5* and no mRNA spanning the insertion site could be detected (Figure 1D). Thus, neither *teb2*
164 nor *teb5* accumulate full length *TEB* mRNA, and are likely knock-out mutants, consistent with
165 previous reports (Inagaki *et al.*, 2006). We next quantified the distribution of *teb* mutants between
166 the two phenotypic categories. In our growth conditions ~ 85-90% of *teb* mutants were in the WTL
167 category and only 10% to 15% in the S category corresponding to the previously described
168 phenotype (Figure 1E).

169 Since *teb* mutants were shown to display a constitutive upregulation of DNA damage responsive
170 genes (Inagaki *et al.*, 2009), we asked whether the severity of the phenotype may correlate with
171 the levels of expression for DDR genes. We thus determined the expression level of *BRCA1* that
172 is involved in the DNA repair and *SMR7* which is an inhibitor of cell cycle progression, in rosette
173 leaves of *teb* plants. Plants from the two phenotypic classes displayed upregulation both genes as
174 previously reported (Inagaki *et al.*, 2009), but no significant differences were observed between
175 *teb* plants with different phenotype (Figure S1).

176 We next asked whether the observed variability in the *teb* mutant phenotype could also be observed
177 earlier during development. Indeed, when analyzing root length of 15-day-old plants, we observed
178 that *teb* mutants displayed a higher proportion of plants with arrested root growth than the wild-
179 type (Figure S2). Likewise, at 10 days after germination, plantlets displayed more variable sizes
180 than the wild-type, with a higher proportion of small plantlets with shorter roots and smaller
181 cotyledons (Figure S3A, B). To determine whether this phenotypic variability related to increased
182 DNA damage accumulation, we performed immuno-labelling of phosphorylated γ -H2AX variant
183 on root tips of wild-type plants and small and big plantlets of *teb* mutants, that forms foci at the

184 site of DSBs (Charbonnel *et al.*, 2010). As shown on Figure 2, we could observe a significant
185 increase in γ -H2AX labelling in *teb* mutants: the percentage of root tip nuclei showing γ -H2AX
186 foci was around 1% in the wild-type, and around 10 % in both *teb* mutant alleles. However, the
187 percentage of labelled nuclei was not significantly different between big and small plantlets.
188 Consistently, DDR genes activation did not differ significantly between small and big *teb* mutants
189 (Figure S3C, D). Furthermore, plants with arrested root growth did not show severe *teb* mutant
190 plants at later stages: we selected 20 of those plantlets and transferred them to the green house, but
191 none of them developed a severe phenotype after 3 weeks. Collectively, these results indicate that
192 loss of Pol θ results in an increase in DNA damage accumulation in proliferating cells, but that the
193 appearance of the *teb* severe phenotype is stochastic, and does not correlate with significantly
194 higher levels of DNA damage or DDR activation.

195 One possible explanation for the stochastic appearance of the severe phenotype in *teb* mutants
196 could be the accumulation of mutations as a consequence of defects in DNA repair. Under such a
197 scenario, developmental defects would be expected to be transmitted to the next generation, or to
198 aggravate in the next generation. To test this, the progeny of WTL and S plants was sown, and we
199 evaluated the distribution of plants between the two classes in the next generation. However, the
200 distribution of plants between the 2 classes was the same in the subsequent generation (Figure S4),
201 suggesting that developmental defects are not due to mutations.

202 **Pol θ is involved in replicative stress tolerance**

203 Pol θ has been proposed to play a key role in replicating cells (Inagaki *et al.*, 2009), we therefore
204 asked whether replicative stress could increase the proportion of plants showing developmental
205 defects in *teb* mutants. Wild-type and *teb* mutants were germinated on MS supplemented with
206 Hydroxyurea (HU, 0.75mM). At 10 days after germination, the survival rate of *teb* mutants was
207 lower than that of wild-type plants (Figure S5), indicating that *teb* mutants are hypersensitive to
208 replicative stress. After 10 days, surviving plants were transferred to soil, and the proportion of
209 plants with a WTL or S phenotype was assessed after 3 weeks. Wild-type (Col-0) plants subjected
210 to this treatment displayed a growth reduction but did not show other developmental defects such
211 as deformed leaves (Figure S6). By contrast, as shown on Figure 1E, the proportion of plants with
212 severe developmental defects was significantly increased in both *teb2* and *teb5* mutants. The

213 proportion of S plants increased from less than 15% to almost 30%, indicating that replicative
214 stress may be the cause for developmental defects observed in *teb* mutants.

215 To further explore the role Pol θ in response to replicative stress, we took advantage of the
216 hypomorphic mutant *pol2a-4*. This mutant (also called *abo4-1*) is partially deficient for the
217 replicative DNA polymerase Pol ϵ (Yin *et al.*, 2009), and we have shown that it displays
218 constitutive replicative stress (Pedroza-Garcia *et al.*, 2017). The *teb2* and *teb5* mutations were
219 therefore introduced in the *pol2a-4* background by crossing, generating the *pol2a teb2* and *pol2a*
220 *teb5* double mutants.

221 Six weeks old plants of all mutant combinations are shown in Figure 3A. Interestingly, *pol2a teb*
222 double mutants displayed severe developmental defects that were fully homogeneous between
223 individuals. To further characterize the developmental defects of *pol2a teb* double mutants, we
224 quantified root length: we observed that *teb* and *pol2a* roots were shorter compared to wild type
225 plants, as previously reported (Inagaki *et al.*, 2006; Pedroza-Garcia *et al.*, 2017). In addition, root
226 length of *pol2a teb* double mutants was significantly reduced compared to single mutants (Figure
227 3B and 3C). Because *teb* mutants display disorganized meristem and spontaneous cell death in
228 root tips (Inagaki *et al.*, 2006), we evaluated whether these defects were exacerbated in *pol2a teb*
229 double mutants. Root tips of eight-day-old plants from mutant combinations were observed by
230 confocal microscopy after propidium iodide staining. We observed disorganized meristem and cell
231 death in the *teb* mutants, confirming the result of the previous study (Inagaki *et al.*, 2006).
232 Furthermore, meristems were severely compromised in *pol2a teb* double mutants (Figure 4A-F)
233 with disorganized patterning, extensive cell death and differentiation of root hair close to the tip
234 of the root. Finally, meristem length was measured in these mutants, showing that *pol2a* and *teb*
235 mutants have smaller root meristem size compared to the wild type Col-0. Moreover, more drastic
236 reduction of meristem size was observed in the *pol2a teb* double mutants (Figure 4G). Finally,
237 *pol2a teb* double mutants accumulated significantly higher levels of γ -H2AX foci than *teb* single
238 mutants, whereas *pol2a* mutants did not accumulate more DSBs than the wild-type, as previously
239 reported ((Pedroza-Garcia *et al.*, 2017), Figure 2D). Together, these results indicate that cell
240 proliferation is more severely compromised in *pol2a teb* double mutants than in parental lines,
241 likely due to increased accumulation of DNA breaks, consistent with the notion that Pol θ plays a
242 key role in the repair of replication-associated DNA damage.

243 Our results indicate that loss of Pol θ impairs the repair of replication-associated DNA damage,
244 which could lead to the activation of the DDR response. To test this hypothesis, we next checked
245 the expression of DNA damage responsive genes in all mutant combinations by qRT-PCR (Figure
246 5). We selected genes representative of different responses triggered by DDR activation such as
247 DNA repair genes (*RAD51* and *BRCA1*) and cell cycle regulation (*SMR5/7*, *WEE1* and *CYCB1*;
248 1). Expression of all tested genes was induced in the *teb* single mutants and in *pol2a* compared to
249 wild-type Col-0, consistent with previous reports (Inagaki *et al.*, 2006; Pedroza-Garcia *et al.*,
250 2017), except for the *WEE1* gene in the *teb5* mutant. Furthermore, these genes displayed an even
251 higher up-regulation in *pol2a teb* than in the single mutants (Figure 5), indicating that replicative
252 stress induced by Pol ϵ deficiency is enhanced by the lack of Pol θ .

253 **Abiotic stresses aggravate the severity of *teb* mutants' phenotype.**

254 Taken together, our results indicate that a key cellular function of Pol θ is to allow repair of
255 replication-associated DNA damage. This led us to postulate that the discrepancies between our
256 observations and previous reports regarding the severity of *teb* mutants' phenotype could stem
257 from different intensities of basal replicative stress between laboratories, due to different growth
258 conditions. Under such a scenario, abiotic stresses would be expected to impact the severity of *teb*
259 mutants' phenotypes. To test this hypothesis, we subjected *teb2* and *teb5* mutants to various abiotic
260 stress conditions: high light intensity (HL, $350 \mu\text{mol} \times \text{m}^{-2} \times \text{s}^{-1}$), salt treatment (50 or 100 mM of
261 NaCl). and heat (growth at 32°C). Except for the HL treatment, plants were grown under a low
262 light intensity (LL, $160 \mu\text{mol} \times \text{m}^{-2} \times \text{s}^{-1}$). After 3 weeks, we counted the plants in each phenotype
263 category ($n > 50$). These treatments obviously modified the phenotype of wild-type plants but did
264 not induce the appearance of the conspicuous *teb*-like phenotype in Col0 plants (Figure S7). It is
265 worth noting that the HL condition could not be considered as a stress condition for wild-type
266 plants as they grew faster and reached a larger size than under LL conditions (Figure S7). The
267 proportion of S plants increased under HL and high salt stress (100mM) for both *teb2* and *teb5*
268 mutants (Figure 6A, B). By contrast, a lower concentration of salt (50mM) had no impact on the
269 distribution of *teb* mutants between the different phenotypic classes. Likewise, growth at 32°C did
270 not significantly affect the proportion of *teb* mutants with a severe phenotype. We tried increasing
271 the temperature to 37°C , but the proportion of plantlets that did not survive in these growth
272 conditions was over 50% in both wild-type and mutants, which prevented further analysis. To

273 determine whether abiotic stress conditions affected the level of DDR activation in *teb* mutants,
274 we monitored the expression of DDR marker genes (Figure S8). Results obtained on mature plants
275 were too variable to draw robust conclusions, so experiments were performed on *in vitro* grown
276 plantlets. The two DNA-repair marker genes (*XRI-1* and *BRCA2*) and the cell cycle inhibitor *SMR7*
277 were induced by salt treatment but not by high-light in wild-type plants, while expression of *SMR5*
278 did not change between growth conditions. All these genes were induced in *teb2* and *teb5* mutants,
279 and reached the same levels under control and high-light conditions. By contrast, all tested DDR
280 marker genes were significantly induced in *teb* mutants grown in the presence of salt compared to
281 control conditions, although the relative expression compared to wild-type plants remained in the
282 same range. These results suggest that salt treatment can lead to DDR activation, and that this
283 phenomenon is amplified in *teb* mutants, consistent with the observation that this treatment leads
284 to an increase in the proportion of plants with a S phenotype. The situation for high-light response
285 appears to be less clear, but it is worth noting that *in vitro* growth conditions may not be fully
286 comparable to growth on soil that we used for plant phenotyping.

287 Together, our results suggest that Pol θ is required in proliferating cells for the repair of replication-
288 induced DNA lesions, and that basal levels of replicative stress vary depending on growth
289 conditions, which likely accounts for the variability of *teb* mutants' phenotype.

290 **DISCUSSION**

291 In mammalian cells, Pol θ mediates both error-prone TLS during DNA replication (Yoon *et al.*,
292 2019; Yousefzadeh and Wood, 2013) and DSB repair through Alt-NHEJ/MMEJ (Beagan and
293 McVey, 2016). This dual role appears to be conserved in plants. Indeed, previous studies have
294 shown that plant Pol θ is required for plant tolerance to various sources of DNA damage:
295 *Arabidopsis* *teb* mutants are hypersensitive to damaging agents such as UV, cisplatin, MMC
296 among others (Inagaki *et al.*, 2006), all of which can induce DNA damage in both proliferating
297 and differentiated cells. More recently, Pol θ was involved in the repair of DSB through Alt-NHEJ
298 (van Kregten *et al.*, 2016; Nishizawa-Yokoi *et al.*, 2020), a process that may also occur both in
299 dividing and in differentiated cells. These observations, together with the fact that Pol θ appeared
300 to be required for normal plant development prompted us to ask whether developmental defects
301 observed in *teb* mutants reflect its function in TLS, DNA repair in all cell types, or repair of

302 replication-associated DNA damage. Here, we were able to show that phenotypic defects triggered
303 by Pol θ deficiency are variable, and that their severity correlates with endogenous replicative
304 stress levels. Indeed, HU treatment increased the proportion of *teb* mutants displaying severe
305 developmental defects. Furthermore, DNA Pol ϵ deficiency that triggers constitutive replicative
306 stress via ATR activation (Pedroza-Garcia *et al.*, 2017) abolished the variability of phenotypic
307 alterations observed in *teb* mutants: *pol2a teb* double mutants all showed the same developmental
308 defects, including drastically reduced growth, loss of primary root meristem function and extensive
309 cell death in the root meristem. We therefore conclude that Pol θ is required for cellular response
310 to replicative stress, and that this cellular function accounts for the developmental defects triggered
311 by Pol θ deficiency. This hypothesis is consistent with the observation that *POLQ* genetically
312 interacts with *ATR* (Inagaki *et al.*, 2009), whose function is to activate the DDR in response to
313 replicative stress: developmental defects of *teb atr* double mutants are drastically enhanced
314 compared to *teb* mutants, and inactivation of ATR prevents upregulation of the DDR marker gene
315 *CYCBI;1* in *teb*. Taken together, these observations indicate that the activity of plant Pol θ is
316 crucial to avoid accumulation of DNA damage during DNA replication in plants. Consistently, in
317 mammals, the Alt-NHEJ activity is maximal during S-phase (Brambati *et al.*, 2020). Likewise,
318 mutations in *Drosophila MUS308* gene induce hypersensitivity to replication-blocking lesions
319 such as inter-strand cross-links (Harris *et al.*, 1996), and Pol θ was shown to play a key role in
320 replication-associated DSB repair (Alexander *et al.*, 2016). A similar finding was reported in
321 *Caenorhabditis elegans*, where loss of Pol θ results in dramatic DNA loss around replication
322 barriers such as G-quadruplexes (Koole *et al.*, 2014). Thus, repair of DNA breaks generated by
323 DNA replication appears to be most prominent cellular function of Pol θ both in plants and
324 animals.

325 Another pending question is how essential this replication-associated DNA repair function is for
326 the normal development of multicellular organisms. The *chaos1* mouse mutants that harbor a point
327 mutation in the *POLQ* gene are viable but show genomic instability, especially in erythrocytes
328 (Shima *et al.*, 2004), but otherwise grow normally. *Drosophila* mutants also do not show major
329 developmental alterations, except for a thin eggshell phenotype (Alexander *et al.*, 2016). In plants,
330 the situation seems less clear as *Arabidopsis teb* mutants grown under our standard laboratory
331 conditions display very variable phenotypic defects, and rice mutants grow and develop normally

332 (Nishizawa-Yokoi *et al.*, 2020). Likewise, in the moss *Physcomitrella patens*, loss of Pol θ does
333 not affect development or genetic stability (Mara *et al.*, 2019). The latter observation may relate
334 to the fact that the most prominent DNA repair pathway in moss cells is homologous
335 recombination (HR) rather than Alt-NHEJ: in *P. patens*, mutants deficient for the RAD51 protein,
336 that is required for HR, show developmental defects and hypersensitivity to DNA damaging agents
337 (Markmann-Mulisch *et al.*, 2007). This suggests that in the moss, replication-associated damage
338 is repaired mainly by HR rather than via Alt-NHEJ. The existence of alternative repair mechanisms
339 also likely accounts for the variability observed in *Arabidopsis teb* mutants' phenotypes. HR, or
340 other back-up repair mechanisms such as canonical NHEJ may compensate for Pol θ deficiency
341 when replicative stress levels are relatively low. However, when the intensity of replicative stress
342 increases, Pol θ becomes indispensable to deal with the accumulating DNA damage, and its
343 absence leads to cell death and developmental defects. Our working model for Pol θ cellular
344 function is summarized on Figure 7: in the wild-type, Pol θ avoids for stalling by promoting TLS,
345 and contributes to the repair of DSBs generated by the combination of fork collapse and
346 converging DNA replication coming from a nearby replication origin. Persistent fork stalling or
347 unrepaired DSBs can activate the DDR via ATR, but this event remains very rare. In the absence
348 of Pol θ , both TLS and DSB repair via Alt-NHEJ are compromised, leading to persistent DNA
349 damage that activates ATR signaling and the DDR. Interestingly, contrasting requirements for Pol
350 θ activity may exist between cell types in higher plants such as *Arabidopsis*. Indeed, Pol θ appears
351 to be strictly required for T-DNA integration when plants are transformed by floral-dip, but not
352 when transformation is done on somatic cells (Nishizawa-Yokoi *et al.*, 2020). The stochastic
353 appearance of severe developmental phenotypes in *teb* mutants, and the fact that they are not
354 heritable through sexual reproduction may be due to the appearance of mutations in somatic cells.
355 Such a hypothesis would imply that meristematic cells that will give rise to the germline rely on
356 other DNA repair pathways than Alt-NHEJ, or are more readily eliminated by programmed cell
357 death than the neighboring initials. A similar situation may exist in animals since in mice, POLQ
358 deficiency affects genomic stability mainly in erythrocytes (Shima *et al.*, 2004).

359 Requirement for Pol θ -dependent DNA repair may differ not only between cell types, but also
360 between genomic regions. In *Drosophila* follicle cells, replication associated damage is repaired
361 preferentially by HR or Pol θ -dependent Alt-NHEJ depending on the loci (Alexander *et al.*, 2016),

362 suggesting that Pol θ -mediated DNA repair is the prevalent DNA repair mechanism after fork
363 collapse only at a subset of genomic regions. Likewise, in Arabidopsis, the *teb* mutations
364 specifically affects the expression of genes with a nearby Helitron as well as that of tandem and
365 dispersed duplicated genes (Inagaki *et al.*, 2009). Authors postulated that the *teb* mutation affects
366 the chromatin state at these loci due to failed HR. One more likely hypothesis would be that Pol θ
367 is preferentially involved in DNA repair at genomic regions that could otherwise engage in
368 illegitimate HR with duplicated loci to avoid loss of genetic information. In the absence of Pol θ ,
369 DNA repair at these genomic regions would be compromised or delayed, which could indeed
370 impair the proper re-establishment of chromatin states after DNA replication. This hypothesis
371 could account for the fact that developmental defects triggered by Pol θ vary in severity and are
372 not transmitted to the next generation through sexual reproduction. Indeed, if developmental
373 defects associated with Pol θ deficiency were due to mutations caused by altered DNA repair, they
374 would be expected to be stochastic in terms of plants' aspect because mutations could occur
375 anywhere in the genome, and heritable. On the contrary, the *teb* mutation gives rise to remarkably
376 similar phenotypical defects that are not heritable, and appear with a variable frequency. Defects
377 in cell cycle progression very likely contribute to these developmental defects. However, it is
378 tempting to speculate that they could also partly be due to changes in gene expression triggered by
379 defects in the restoration of chromatin states after DNA replication. If Pol θ is preferentially
380 involved in DNA repair at specific genomic contexts, this model would also explain why plants
381 with severe developmental defects all look identical.

382 Finally, our results not only provide evidence for the role of Pol θ during DNA replication, but
383 also reveal that abiotic stresses can enhance the requirement for Pol θ , indicating that levels of
384 replicative stress in dividing cells may differ depending on growth conditions. How abiotic stresses
385 affect genome integrity in plants remains to be fully elucidated (Nisa *et al.*, 2019). The effect of
386 UV light or heavy metals on DNA is well documented (Chen *et al.*, 2019), but the consequences
387 of other stresses such as temperature changes, drought, salinity or light intensity have been less
388 explored, although there is accumulating evidence that DDR signaling may be a relevant element
389 in plants' response to these stimuli. Indeed, the ANAC044 and ANAC085 transcription factors,
390 that are activated by DNA damage also contribute to the induction of a G2-arrest in response to
391 heat stress (Takahashi *et al.*, 2019). Whether their role reflects the accumulation of DNA damage

392 in response to heat, or the recruitment of this DDR branch to respond to heat stress remains to be
393 clarified, but these results suggest that DDR signaling may play a more prominent role than
394 previously anticipated in plants' response to environmental stresses. In line with this hypothesis,
395 root meristem maintenance under chilling conditions requires DDR signaling components (Hong
396 *et al.*, 2017). Our results indicate that at least high light and salt may induce replicative stress in
397 plants, as evidenced by the aggravation of *teb* mutants' phenotypes. By contrast, we could not
398 detect any effect of heat stress. This may be due to the fact that we exposed plants to a slightly less
399 severe heat stress than Takahashi and colleagues (Takahashi *et al.*, 2019) because prolonged
400 growth at 37°C resulted in a high mortality rate in both wild-type and mutant plants. However, this
401 could also mean that all types of abiotic stresses do not affect DNA replication in the same way.
402 Future work should help elucidate how much mechanisms involved in the maintenance of genome
403 integrity contribute to plants developmental plasticity in response to stress, and whether different
404 stress conditions affect genome integrity in different ways.

405

406 MATERIAL AND METHODS

407 Plant material and growth conditions

408 All *Arabidopsis thaliana* mutants used in this study are in the wild type Columbia-0 (Col-0)
409 background. *teb2* (SALK_035610) and *teb5* (SALK_018851) mutants were a kind gift from M.
410 van Kregten (Leiden University).

411 Seeds were surface sterilized and treated with bayrochlore™ for 20 min, then washed with sterile
412 water and kept at 4°C for 2 days. They were next sown on commercially available 0.5× Murashige
413 and Skoog (MS, Duchefa) medium solidified with 0.8% agar (Phyto-Agar HP696, Kalys). Plates
414 were then transferred to a long day (16 h light, 8 h night, 21°C) *in vitro* growth chamber. After 2
415 weeks plants were transferred to soil under short day conditions (8 h light 20°C, 16 h night at 18°C)
416 for one week and after that transferred to a long day growth chamber (16 h light, 8 h night, 21°C)
417 for phenotypic analysis.

418 Genotyping of the *teb2* and *teb5* mutants was performed using the Lba1/RP primer combination
419 for the mutant allele and the LP/RP primer combination for the wild-type allele. Sequence of
420 primers used can be found in Table S1.

421 **Genotoxic test**

422 Wild type Col-0 and *teb* mutants *teb2* and *teb5*) were germinated on MS medium (Control
423 condition) and some were germinated on MS supplemented hydroxyurea (HU) concentration was
424 0.75 mM. After 2 weeks, these mutant plants were transferred to soil. Then after 10 days, the
425 survival rate of these plants was measured.

426 **RNA extraction and quantitative RT-PCR**

427 Total RNA was extracted from flower buds using NucleoSpin® RNA protocol (MACHEREY-
428 NAGEL). First strand cDNA was synthesized from 2µg of total RNAs by using ImProm-II™
429 Reverse Transcription System (Promega) according to the manufacturer's instructions. 1/50th of
430 the synthesized cDNA was mixed with 100nM of each primer and LightCycler 480 Sybr Green I
431 mastermix (Roche Applied Science) for quantitative PCR analysis. Products were amplified and
432 fluorescent signals acquired with a LightCycler 480 detection system. The specificity of
433 amplification products was determined by melting curves. Data were from triplicates and are
434 representative of at least two biological replicates. The sequence of primers used in this study is
435 provided in Supplementary Table 1. DDR-related genes expressions were normalized by using
436 housekeeping gene *ACTIN*. Similar results were observed in 3 independent experiments.

437

438 **Immuno-fluorescence**

439 Immuno-labelling of γ -H2AX foci was performed as described previously (Charbonnel *et al.*,
440 2010). Slides were imaged with an epifluorescence microscope (AxioImager Z.2; Carl Zeiss) fitted
441 with a metal halide lamp and the appropriate shifted free filter sets for imaging DAPI and Alexa
442 488 dyes. Images were acquired with a cooled CCD camera (AxioCam 506 monochrome; Carl
443 Zeiss) operated using Zen Blue software (Carl Zeiss).

444

445 **Confocal microscopy imaging**

446 Root tips of 8-day-old plantlets were stained with propidium iodide (PI, 10 μ M) and then root
447 meristems were observed using 20X water immersion lens on a Zeiss LSM 880 laser scanning
448 confocal microscope using a 561nm laser for excitation. Fluorescence was acquired between 565
449 nm and 700 nm. Representative images were collected from 10 to 15 roots with three biological
450 replicates.

451 **Abiotic stress**

452 In this study three different abiotic stress were applied on *teb* mutants. These mutant seeds were
453 grown on 1/2 MS medium and germinated *in vitro* and after 10 days transferred to pots (soil).
454 Control plants were kept at 20°C under low light intensity (LL, 160 μ mol x m⁻² x s⁻¹), and watered
455 with water. Plants were either subjected to high light intensity (HL, 350 μ mol x m⁻² x s⁻¹) at 20°C,
456 or transferred in a growth cabinet at 32°C (16h day, 8h night, 28°C at night) under LL or kept at
457 20°C under LL but watered with two NaCl solutions (50mM or 100mM). For the higher salt
458 concentration, plants were first watered with NaCl for 3 days, and the concentration was then
459 increased to 100mM. Distribution of plants between the three phenotypic classes was documented
460 after three weeks of these stresses. Chi-squared tests was used to compare the distributions between
461 phenotypic classes. Experiments were performed twice giving similar results.

462 **Accession numbers**

463 Accession numbers of the genes mentioned in this study are as follows: *TEBICHI* (AT4G32700),
464 *POL2A* (AT1G08260), *CYCB1;1* (AT4G37490), *RAD51* (AT5G20850), *WEE1* (AT1G02970),
465 *BRCA2* (AT1G80210), *SMR5* (AT1G07500), *SMR7* (AT3G27630).

466 **Acknowledgements**

467 Maherun Nisa is supported by a grant from the Fondation pour la Recherche Médicale
468 (ECO201806006824). We thank Marleen van Kregten for providing the seeds of the *teb* mutants
469 and Charles White (GReD, Clermont-Ferrand) for the kind gift of the anti γ -H2AX antibody. We
470 thank Maxence Remerand and Lazare Brezillon-Dubus, who helped characterizing *pol2a teb*
471 double mutants during their internship. The present work has benefited from the core imaging
472 facilities of IPS2 supported by the Labex ‘Saclay PlantScience’ (ANR-11-IDEX-0003-02).

473 **Conflict of interest**

474 Authors declare no conflict of interest.

475

476 REFERENCES

477 **Adachi, S., Minamisawa, K., Okushima, Y., et al.** (2011) Programmed induction of
478 endoreduplication by DNA double-strand breaks in Arabidopsis. *Proc Natl Acad Sci U S A*,
479 **108**, 10004–10009. Available at: <http://www.ncbi.nlm.nih.gov/pubmed/21613568>.

480 **Alexander, J.L., Beagan, K., Orr-Weaver, T.L. and McVey, M.** (2016) Multiple mechanisms
481 contribute to double-strand break repair at rereplication forks in Drosophila follicle cells.
482 *Proc. Natl. Acad. Sci. U. S. A.*, **113**, 13809–13814. Available at:
483 <http://www.ncbi.nlm.nih.gov/pubmed/27849606> [Accessed June 17, 2020].

484 **Beagan, K. and McVey, M.** (2016) Linking DNA polymerase theta structure and function in
485 health and disease. *Cell. Mol. Life Sci.*, **73**, 603–15. Available at:
486 <http://www.ncbi.nlm.nih.gov/pubmed/26514729> [Accessed June 16, 2020].

487 **Brambati, A., Barry, R.M. and Sfeir, A.** (2020) DNA polymerase theta (Polu)-an error-prone
488 polymerase necessary for genome stability. *Curr Opin Genet Dev*, **60**, 119–126. Available
489 at: <https://doi.org/10.1016/j.gde.2020.02.017>.

490 **Burgers, P.M.J.** (1998) Eukaryotic DNA polymerases in DNA replication and DNA repair.
491 *Chromosoma*.

492 **Charbonnel, C., Gallego, M.E. and White, C.I.** (2010) Xrcc1-dependent and Ku-dependent
493 DNA double-strand break repair kinetics in Arabidopsis plants. *Plant J.*, **64**, 280–290.
494 Available at: <http://www.ncbi.nlm.nih.gov/pubmed/21070408> [Accessed October 14, 2015].

495 **Chen, P., Sjogren, C.A., Larsen, P.B. and Schnittger, A.** (2019) A multi-level level response
496 to DNA damage induced by Aluminium. *Plant J.*, **98**, 479-491.

497 **Chiruvella, K.K., Liang, Z. and Wilson, T.E.** (2013) Repair of double-strand breaks by end
498 joining. *Cold Spring Harb. Perspect. Biol.*, **5**, a012757. Available at:
499 <http://www.ncbi.nlm.nih.gov/pubmed/23637284> [Accessed June 16, 2020].

500 **Ciccia, A. and Elledge, S.J.** (2010) The DNA Damage Response: Making It Safe to Play with
501 Knives. *Mol. Cell*.

502 **Feng, W., Simpson, D.A., Carvajal-Garcia, J., et al.** (2019) Genetic determinants of cellular
503 addiction to DNA polymerase theta. *Nat. Commun.*, **10**, 1–13. Available at:
504 <https://doi.org/10.1038/s41467-019-12234-1> [Accessed October 26, 2020].

505 **Fulcher, N. and Sablowski, R.** (2009) Hypersensitivity to DNA damage in plant stem cell
506 niches. *Proc Natl Acad Sci U S A*, **106**, 20984–20988. Available at:
507 [http://www.ncbi.nlm.nih.gov/entrez/query.fcgi?cmd=Retrieve&db=PubMed&dopt=Citation](http://www.ncbi.nlm.nih.gov/entrez/query.fcgi?cmd=Retrieve&db=PubMed&dopt=Citation&list_uids=19933334)
508 [&list_uids=19933334](http://www.ncbi.nlm.nih.gov/entrez/query.fcgi?cmd=Retrieve&db=PubMed&dopt=Citation&list_uids=19933334).

509 **Harris, P. V, Mazina, O.M., Leonhardt, E.A., Case, R.B., Boyd, J.B. and Burtis, K.C.**
510 (1996) Molecular cloning of Drosophila mus308, a gene involved in DNA cross-link repair
511 with homology to prokaryotic DNA polymerase I genes. *Mol. Cell. Biol*.

512 **Hong, J.H., Savina, M., Du, J., Devendran, A., Kannivadi Ramakanth, K., Tian, X., Sim,**
513 **W.S., Mironova, V. V. and Xu, J.** (2017) A Sacrifice-for-Survival Mechanism Protects
514 Root Stem Cell Niche from Chilling Stress. *Cell*, **170**, 102-113.e14. Available at:
515 <http://www.ncbi.nlm.nih.gov/pubmed/28648662> [Accessed November 18, 2018].

516 **Hu, Z., Cools, T. and Veylder, L. De** (2016) Mechanisms Used by Plants to Cope with DNA
517 Damage. *Annu. Rev. Plant Biol.*, **67**, 439–62. Available at:
518 <http://www.ncbi.nlm.nih.gov/pubmed/26653616> [Accessed July 14, 2016].

519 **Inagaki, S., Nakamura, K. and Morikami, A.** (2009) A link among DNA replication,
520 recombination, and gene expression revealed by genetic and genomic analysis of TEBICHI
521 gene of Arabidopsis thaliana P. S. Schnable, ed. *PLoS Genet*, **5**, e1000613. Available at:
522 <https://dx.plos.org/10.1371/journal.pgen.1000613> [Accessed July 30, 2019].

523 **Inagaki, S., Suzuki, T., Ohto, M., Urawa, H., Horiuchi, T., Nakamura, K. and Morikami,**
524 **A.** (2006) Arabidopsis TEBICHI, with helicase and DNA polymerase domains, is required
525 for regulated cell division and differentiation in meristems. *Plant Cell*, **18**, 879–92.
526 Available at: <http://www.ncbi.nlm.nih.gov/pubmed/16517762> [Accessed July 30, 2019].

527 **Jain, R., Aggarwal, A.K. and Rechkoblit, O.** (2018) Eukaryotic DNA polymerases. *Curr.*
528 *Opin. Struct. Biol.*, **53**, 77–87. Available at:
529 <http://www.ncbi.nlm.nih.gov/pubmed/30005324> [Accessed February 12, 2019].

530 **Koole, W., Schendel, R. Van, Karambelas, A.E., Heteren, J.T. Van, Okihara, K.L. and**
531 **Tijsterman, M.** (2014) A polymerase theta-dependent repair pathway suppresses extensive
532 genomic instability at endogenous G4 DNA sites. *Nat. Commun.*, **5**. Available at:
533 <https://pubmed.ncbi.nlm.nih.gov/24496117/> [Accessed October 31, 2020].

534 **Kregten, M. van, Pater, S. de, Romeijn, R., Schendel, R. van, Hooykaas, P.J.J. and**
535 **Tijsterman, M.** (2016) T-DNA integration in plants results from polymerase- θ -mediated
536 DNA repair. *Nat. Plants*, **2**, 16164. Available at:
537 <http://www.nature.com/articles/nplants2016164> [Accessed July 30, 2019].

538 **Kunkel, T.A.** (2004) DNA replication fidelity. *J. Biol. Chem.*, **279**, 16895–8. Available at:
539 <http://www.ncbi.nlm.nih.gov/pubmed/14988392> [Accessed February 12, 2019].

540 **Makarova, K.S. and Koonin, E. V** (2013) Archaeology of eukaryotic DNA replication. *Cold*
541 *Spring Harb. Perspect. Biol.*, **5**, a012963. Available at:
542 <http://cshperspectives.cshlp.org/lookup/doi/10.1101/cshperspect.a012963> [Accessed
543 September 9, 2019].

544 **Mara, K., Charlot, F., Guyon-Debast, A., Schaefer, D.G., Collonnier, C., Grelon, M. and**
545 **Nogu e, F.** (2019) POLQ plays a key role in the repair of CRISPR/Cas9-induced double-
546 stranded breaks in the moss *Physcomitrella patens*. *New Phytol.*

547 **Markmann-Mulisch, U., Wendeler, E., Zobell, O., Schween, G., Steinbiss, H.H. and Reiss,**
548 **B.** (2007) Differential requirements for RAD51 in *Physcomitrella patens* and *Arabidopsis*
549 *thaliana* development and DNA damage repair. *Plant Cell*, **19**, 3080–3089. Available at:
550 <https://pubmed.ncbi.nlm.nih.gov/17921313/> [Accessed October 31, 2020].

551 **Mateos-Gomez, P.A., Kent, T., Deng, S.K., McDevitt, S., Kashkina, E., Hoang, T.M.,**
552 **Pomerantz, R.T. and Sfeir, A.** (2017) The helicase domain of Pol θ counteracts RPA to
553 promote alt-NHEJ. *Nat. Struct. Mol. Biol.*, **24**, 1116–1123. Available at:
554 <http://www.ncbi.nlm.nih.gov/pubmed/29058711> [Accessed June 16, 2020].

555 **Nisa, M.-U., Huang, Y., Benhamed, M. and Raynaud, C.** (2019) The Plant DNA Damage
556 Response: Signaling Pathways Leading to Growth Inhibition and Putative Role in Response
557 to Stress Conditions. *Front. Plant Sci.*, **10**, 653. Available at:
558 <http://www.ncbi.nlm.nih.gov/pubmed/31164899> [Accessed July 28, 2019].

559 **Nishizawa-Yokoi, A., Saika, H., Hara, N., Lee, L., Toki, S. and Gelvin, S.B.** (2020)
560 *Agrobacterium* T-DNA integration in somatic cells does not require the activity of DNA
561 polymerase theta. *New Phytol.*, nph.17032. Available at:
562 <https://onlinelibrary.wiley.com/doi/10.1111/nph.17032> [Accessed October 31, 2020].

563 **Noctor, G. and Foyer, C.H.H.** (2016) Intracellular Redox Compartmentation and ROS-Related
564 Communication in Regulation and Signaling. *Plant Physiol.*, **171**, 1581–92. Available at:
565 <http://www.ncbi.nlm.nih.gov/pubmed/27208308> [Accessed March 6, 2019].

566 **Pedroza-Garcia, J.-A., Veylder, L. De and Raynaud, C.** (2019) Plant DNA Polymerases. *Int.*
567 *J. Mol. Sci.*, **20**. Available at: <http://www.ncbi.nlm.nih.gov/pubmed/31569730> [Accessed
568 June 16, 2020].

569 **Pedroza-Garcia, J.A., Mazubert, C., Olmo, I. Del, et al.** (2017) Function of the plant DNA
570 Polymerase epsilon in replicative stress sensing, a genetic analysis. *Plant Physiol.*, **173**,
571 1735-1749.

572 **Powers, K.T. and Washington, M.T.** (2018) Eukaryotic translesion synthesis: Choosing the
573 right tool for the job. *DNA Repair (Amst.)*, **71**, 127–134. Available at:
574 <https://www.sciencedirect.com/science/article/pii/S1568786418301812?via%3Dihub>
575 [Accessed February 12, 2019].

576 **Sakamoto, A.N.** (2019) Translesion Synthesis in Plants: Ultraviolet Resistance and Beyond.
577 *Front. Plant Sci.*, **10**, 1208. Available at: www.frontiersin.org [Accessed November 18,
578 2020].

579 **Shima, N., Munroe, R.J. and Schimenti, J.C.** (2004) The mouse genomic instability mutation
580 chaos1 is an allele of Polq that exhibits genetic interaction with Atm. *Mol. Cell. Biol.*, **24**,
581 10381–9. Available at: <http://www.ncbi.nlm.nih.gov/pubmed/15542845> [Accessed June 17,
582 2020].

583 **Takahashi, N., Ogita, N., Takahashi, T., Taniguchi, S., Tanaka, M., Seki, M. and Umeda,**
584 **M.** (2019) A regulatory module controlling stress-induced cell cycle arrest in Arabidopsis.
585 *Elife*, **8**. Available at: <http://www.ncbi.nlm.nih.gov/pubmed/30944065> [Accessed April 24,
586 2019].

587 **Wang, Z., Song, Y., Li, S., Kurian, S., Xiang, R., Chiba, T. and Wu, X.** (2019) DNA
588 polymerase (POLQ) is important for repair of DNA double-strand breaks caused by fork
589 collapse. *J. Biol. Chem.*, **294**, 3909–3919. Available at:
590 </pmc/articles/PMC6422074/?report=abstract> [Accessed October 31, 2020].

591 **Yang, W. and Gao, Y.** (2018) Translesion and Repair DNA Polymerases: Diverse Structure and
592 Mechanism. *Annu. Rev. Biochem.*, **87**, 239–261. Available at:
593 <https://www.annualreviews.org/doi/10.1146/annurev-biochem-062917-012405> [Accessed
594 September 9, 2019].

595 **Yin, H., Zhang, X., Liu, J., Wang, Y., He, J., Yang, T., Hong, X., Yang, Q. and Gong, Z.**
596 (2009) Epigenetic regulation, somatic homologous recombination, and abscisic acid
597 signaling are influenced by DNA polymerase epsilon mutation in Arabidopsis. *Plant Cell*,
598 **21**, 386–402. Available at: <http://www.ncbi.nlm.nih.gov/pubmed/19244142>.

599 **Yoon, J.-H., McArthur, M.J., Park, J., Basu, D., Wakamiya, M., Prakash, L. and Prakash,**
600 **S.** (2019) Error-Prone Replication through UV Lesions by DNA Polymerase θ Protects
601 against Skin Cancers. *Cell*, **176**, 1295-1309.e15. Available at:
602 <http://www.ncbi.nlm.nih.gov/pubmed/30773314> [Accessed June 17, 2020].

603 **Yoshiyama, K.O., Kobayashi, J., Ogita, N., Ueda, M., Kimura, S., Maki, H. and Umeda, M.**
604 (2013) ATM-mediated phosphorylation of SOG1 is essential for the DNA damage response
605 in Arabidopsis. *EMBO Rep*, **14**, 817–822. Available at:
606 <http://www.ncbi.nlm.nih.gov/pubmed/23907539>.

607 **Yousefzadeh, M.J. and Wood, R.D.** (2013) DNA polymerase POLQ and cellular defense
608 against DNA damage. *DNA Repair (Amst.)*, **12**, 1–9. Available at:
609 </pmc/articles/PMC3534860/?report=abstract> [Accessed November 18, 2020].

610 **Zeman, M.K. and Cimprich, K.A.** (2014) Causes and consequences of replication stress. *Nat.*

612

613 **Figure Legends**

614 **Figure 1: The *tebichi* mutation results in variable developmental defects that can be enhanced** 615 **by replicative stress**

616 A: Representative phenotypes observed in *teb-2* and *teb-5* homozygous mutants after 1 month of
617 growth on soil. Plants were classified in 3 categories: wild-type like (WT), intermediate (I) with
618 only mild growth reduction and a few deformed or twisted leaves (arrowhead), or severe (S) with
619 clear growth reduction and abnormal leaf shape. Bar = 1cm.

620 B: Structure of the *POLQ* gene and position of the T-DNA insertions in the *teb2* and *teb5* alleles.
621 Exons are indicated by grey boxes and introns by a grey line. Primers used for genotyping are
622 indicated by arrows.

623 C: Result of genotyping for *teb* mutants with wild-type-like (WTL) or severe (S) phenotype. Both
624 types of plants were found to be homozygous for the *teb* mutation.

625 D: qPCR quantification of *POLQ* expression in *teb* mutants. Actin was used for normalization.
626 The position of primer pairs is indicated by corresponding numbers.

627 E: Distribution of *teb* mutants between the three phenotypic classes with and without HU
628 treatment. Plants were germinated on control (MS) or hydroxyurea supplemented medium (HU)
629 to a final concentration of 0.75mM. They were transferred to soil after 12 days, and phenotypes
630 were observed after one month. Asterisks denote significant differences between distributions
631 (Chi-squared test, $p < 0.01$). Blind scoring was performed on wild-type and *teb* mutants, the
632 proportion of severe phenotypes observed in wild-type plants was below 2% in all conditions.

633

634 **Figure 2: *teb* mutants show DSB accumulation in root meristems**

635 A-C: representative images of *teb2* root tip nuclei after g-H2AX immuno-staining (A: DAPI
636 fluorescence, B: Alexa 488 fluorescence, C: merged image). Bar = 10 μ m, arrows indicate nuclei
637 with g-H2AX foci. D: quantification of γ -H2AX foci in the indicated genotypes ($n > 1500$ nuclei
638 imaged from 10 root tips for all genotypes). Different letters indicate statistically different values,

639 ANOVA followed by a post-hoc Tukey test $p < 0.01$). Data are representative of 2 biological
640 replicates.

641

642 **Figure 3: Constitutive replicative stress aggravates the phenotype of *teb* mutants**

643 A: Phenotype of the wild-type (Col0), *teb-2*, *teb-5*, *pol2a-4*, *pol2a teb2* and *pol2a teb5* mutants
644 after 40 days of growth under standard conditions ($160 \mu\text{mol photon} \times \text{m}^{-2}\text{xs}^{-1}$, 16h light, 20°C).
645 Bar = 1cm.

646 B: Root length of the wild-type (Col0), *teb-2*, *teb-5*, *pol2a-4*, *pol2a teb2* and *pol2a teb5*. Plants
647 were grown vertically *in vitro* for one week.

648 C: Quantification of the root length in the different genotypes. Data are from at least 20
649 measurements for each line and are representative of 2 independent experiments. Different letters
650 indicate statistically significant differences (ANOVA and Tukey test $p < 0.01$).

651

652 **Figure 4: The root meristem of *teb pol2a* double mutants is severely compromised**

653 A-F: Confocal images of root tips of 8-day-old plants stained with propidium iodide. A: WT
654 (Col0), B: *teb2*, C: *teb5*, D: *pol2a-4*, E: *pol2a teb2* F: *pol2a teb5*. The meristem of *teb* mutants
655 showed abnormal organization and cell death. This defect was exacerbated in *pol2a teb* double
656 mutants with root hair differentiating close to the root tip and meristem organization being
657 dramatically altered. Red arrow indicates the limit of the root apical meristem. Bar = $50\mu\text{m}$ for all
658 panels.

659 G: Meristem length was measured in all mutant combinations. Values are from at least 10 roots
660 and are representative of two independent experiments. Different letters indicate statistically
661 significant differences (ANOVA and Tukey test $p < 0.01$).

662

663 **Figure 5: DDR genes are hyper-induced in *teb pol2a* double mutants**

664 Total RNA was extracted from twelve-day-old plantlets. Expression of selected genes was
665 assessed by real-time qPCR and normalized to actin. We monitored the expressions of genes
666 involved in cell-cycle arrest (*SMR5*, *SMR7* and *WEE1*), DNA repair (*RAD51* and *BRCA2*) and both
667 (*CYCB1;1*). Values are Fold change compared to the wild-type Col-0. Graphs represent average
668 of 3 technical replicates +/- standard deviation and are representative of 3 independent biological

669 replicates. Different letters above bars denote statistically relevant differences (ANOVA followed
670 by Tukey test, performed on raw data before normalization, $p < 0.01$).

671

672 **Figure 6: Some abiotic stresses aggravate the developmental defects of *teb* mutants.**

673 A: Distribution of *teb* mutants between the different classes in plants grown in low light (LL,
674 $160\mu\text{mol} \times \text{m}^{-2} \times \text{s}^{-1}$) or high light (HL, $350\mu\text{mol} \times \text{m}^{-2} \times \text{s}^{-1}$).

675 B: Distribution of *teb* mutants between the different classes in plants grown at standard
676 temperature (20°C) or under heat stress (32°C). Plants were germinated *in vitro* and transferred to
677 soil after 10 days. After 3 days of growth under control conditions at $160\mu\text{mol} \times \text{m}^{-2} \times \text{s}^{-1}$ plants
678 were kept under the same conditions or transferred to 32°C under the same light intensity.

679 C: Distribution of *teb* mutants between the different classes in plants watered with or without salt
680 to the indicated concentration. Plants were germinated *in vitro* and transferred to soil after 10 days.
681 After 3 days of growth under control conditions ($160\mu\text{mol} \times \text{m}^{-2} \times \text{s}^{-1}$, 20°C , salt-treated plants
682 were watered with a solution containing NaCl (50mM), for the 100mM treatment, salt
683 concentration was increased to 100mM after 2days.

684 For all panels, n.s. indicates non-significant differences and asterisks denote significant
685 differences between distributions (Chi-squared test, $p < 0.01$). Blind scoring was performed on wild-
686 type and *teb* mutants in all growth conditions, the proportion of severe phenotypes observed in wild-
687 type plants was below 2%.

688

689 **Figure 7: Model for the role of Pol θ during replicative stress response**

690 A: In the wild-type, replication blocking lesions induce fork stalling. Pol θ can allow TLS through
691 some lesions such as pyrimidine dimers. If efficient lesion bypass cannot be achieved, replisome
692 disassembly and persistent fork stalling activates the DDR through ATR signalling, and DNA
693 synthesis from a converging fork can lead to the formation of a double-ended DSB. Pol θ
694 contributes to the repair of these lesions through Alt-NHEJ but other pathways such as HR or
695 NHEJ likely contribute to DSB repair. B: In the absence of Pol θ , TLS through some lesions is
696 compromised, leading to an increased frequency of fork collapse and persistent stalling.
697 Furthermore, Alt-NHEJ is also compromised; leading to an increased frequency of failed repair,
698 constitutive activation of the DDR through ATR signalling, cell death and stochastic

699 developmental defects. Abiotic stress and replicative stress can modify this equilibrium by
700 enhancing the accumulation of more replication-blocking lesions, leading to an increased
701 frequency of developmental defects in Pol θ deficient lines.

702

703 **Supplemental Figures**

704 **Figure S1: Levels of DDR genes induction do not correlate with the severity of *teb* mutants’**
705 **phenotype.**

706 **Figure S2: Root growth defects show some heterogeneity in *teb* mutants**

707 **Figure S3: Heterogeneous phenotypes of *teb* mutant plantlets do not correlate with different**
708 **levels of DDR genes activation**

709 **Figure S4: The *teb* phenotype does not aggravate over generations**

710 **Figure S5: *teb* mutants are hypersensitive to replicative stress**

711 **Figure S6: Representation phenotypes of wild-type (Col0) and *teb* mutants exposed to HU**
712 **before transfer to the green house**

713 **Figure S7: Representation phenotypes of wild-type (Col0) and *teb* mutants grown under**
714 **different conditions.**

715 **Figure S8: Salt treatment, but not increasing light intensity activates DDR gene expression**
716 **in both wild-type and *teb* mutants.**

717

718

719 **Supplemental Tables**

720 **Table S1: Primer sequences**

721

722

723

724

725

726

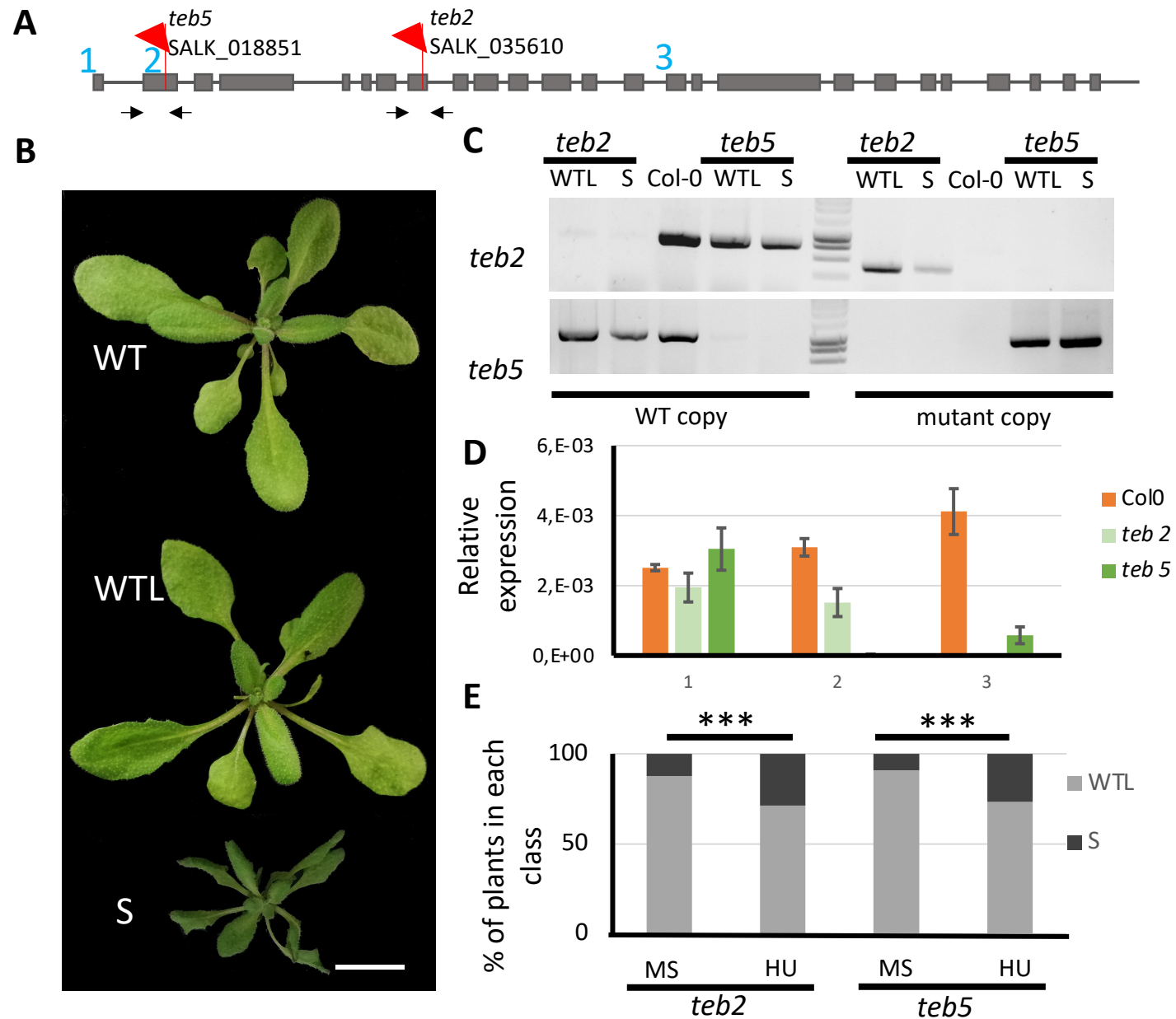


Figure 1. The *tebichi* mutation results in variable developmental defects that can be enhanced by replicative stress

A: Structure of the *POLQ* gene and position of the T-DNA insertions in the *teb2* and *teb5* alleles. Exons are indicated by grey boxes and introns by a grey line. Primers used for genotyping are indicated by arrows. **B:** Representative phenotypes observed in *teb-2* and *teb-5* homozygous mutants after 1 month of growth on soil. Plants were classified in 2 categories: wild-type like (WT) and severe (S) with clear growth reduction and abnormal leaf shape. Bar = 1cm. **C:** Result of genotyping for *teb* mutants with wild-type-like (WTL) or severe (S) phenotype. Both types of plants were found to be homozygous for the *teb* mutation. **D:** qPCR quantification of *POLQ* expression in *teb* mutants. Actin was used for normalization. The position of primer pairs is indicated by corresponding numbers in (A). Data are average \pm S.D. of three technical replicates and representative of three independent experiments. **E:** Distribution of *teb* mutants between the two phenotypic classes with and without HU treatment. Plants were germinated on control (MS) or hydroxyurea supplemented medium (HU) to a final concentration of 0.75 mM. They were transferred to soil after 12 days, and phenotypes were observed after one month ($n > 50$). Asterisks denote statistically relevant differences between distributions (χ^2 -test, $p < 0.01$). Blind scoring was performed on wild-type and *teb* mutants, the proportion of severe phenotypes observed in wild-type plants was below 2% in all conditions.

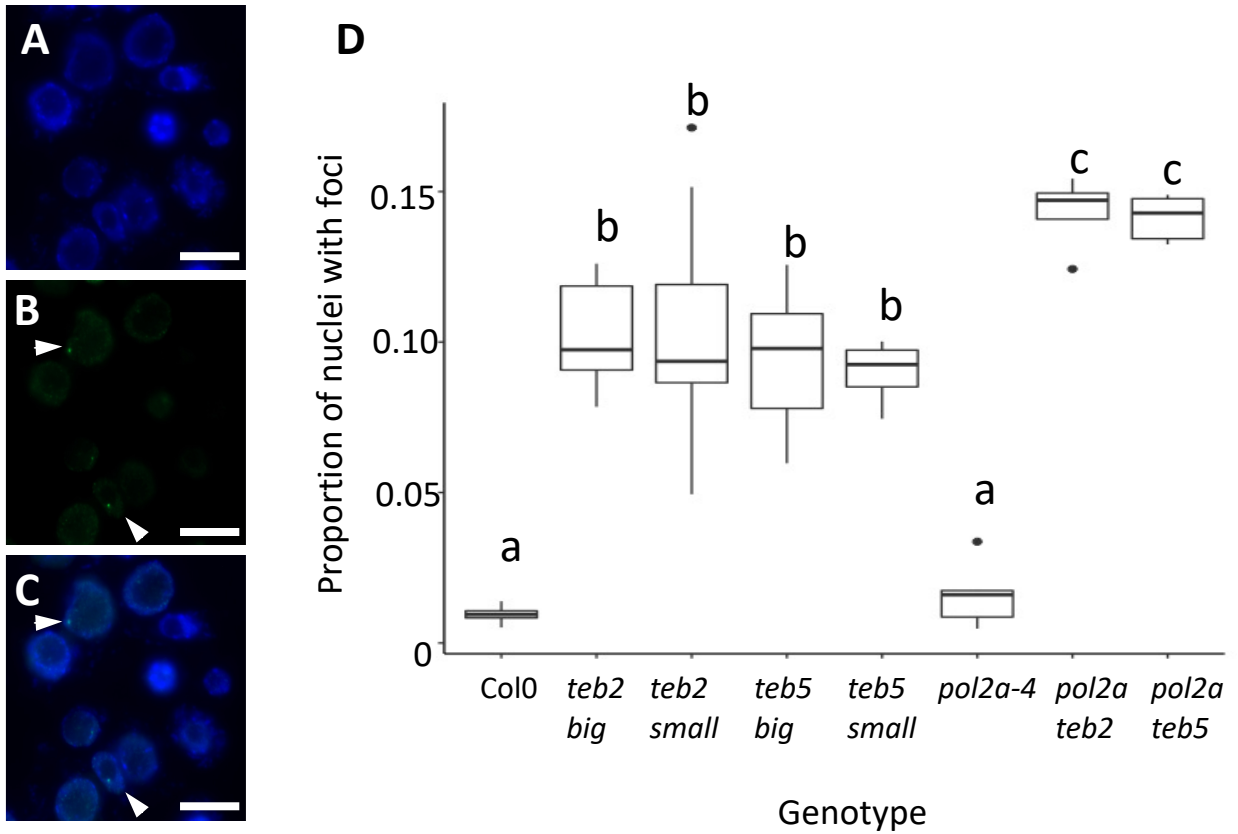


Figure 2. *teb* mutants show DSB accumulation in root meristems

A-C: representative images of *teb2* root tip nuclei after γ -H2AX immuno-staining (A: DAPI fluorescence, B: Alexa 488 fluorescence, C: merged image). Bar = 10 μ m, arrows indicate nuclei with γ -H2AX foci. D: quantification of γ -H2AX foci in the indicated genotypes ($n > 1500$ nuclei imaged from 10 root tips for all genotypes). Different letters indicate statistically different values, ANOVA followed by a post-hoc Tukey test $p < 0.01$). Data are representative of 2 biological replicates.

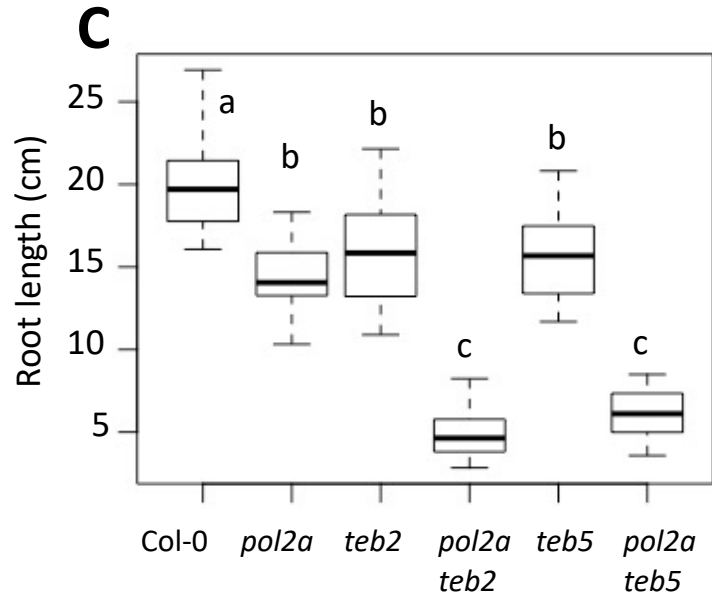
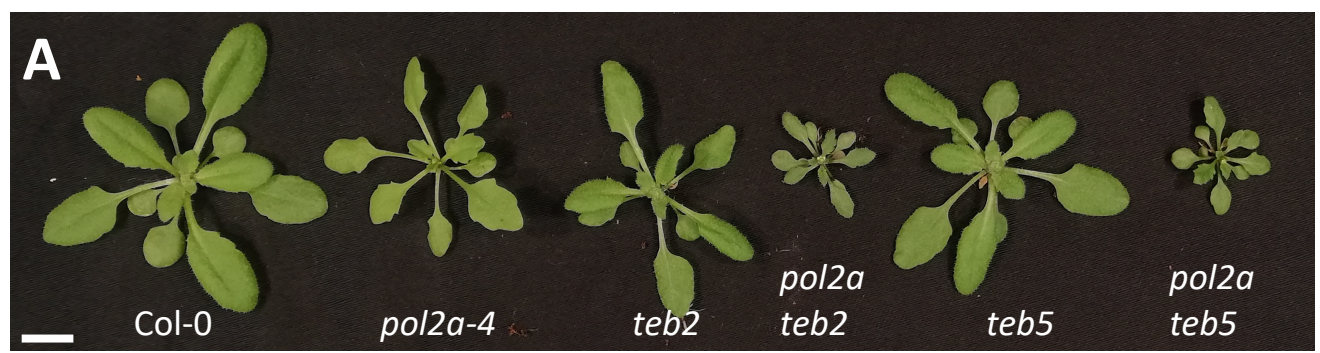


Figure 3. Constitutive replicative stress aggravates the phenotype of *teb* mutants

A: Phenotype of the wild-type (Col0), *teb-2*, *teb-5*, *pol2a-4*, *pol2a teb2* and *pol2a teb5* mutants after 40 days of growth under standard conditions ($160 \mu\text{mol photon} \times \text{m}^{-2}\text{xs}^{-1}$, 16h light, 20°C). Bar = 1 cm.

B: Root length of the wild-type (Col0), *teb-2*, *teb-5*, *pol2a-4*, *pol2a teb2* and *pol2a teb5*. Plants were grown vertically *in vitro* for one week.

C: Quantification of the root length in the different genotypes. Data are from at least 20 measurements for each line and are representative of 2 independent experiments. Different letters indicate statistically relevant differences (ANOVA and Tukey test $p < 0.01$).

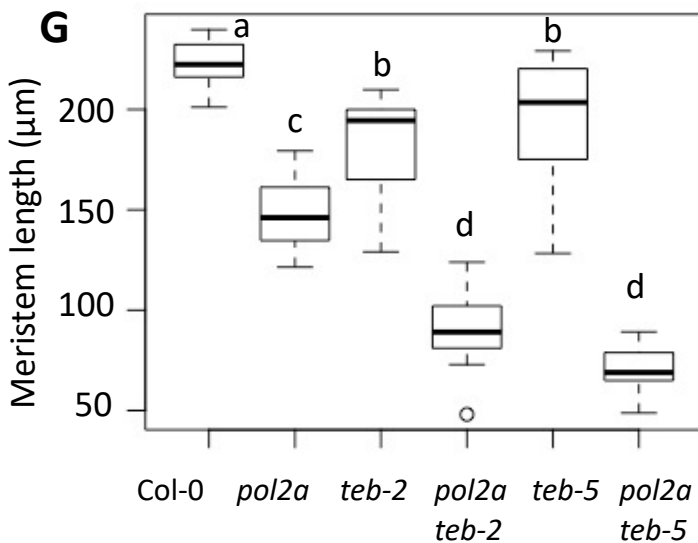
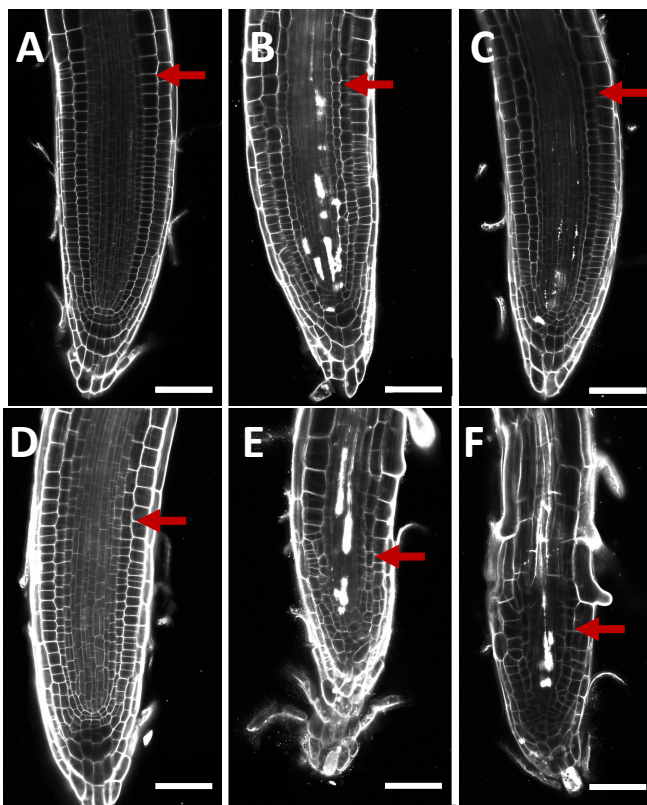


Figure 4. The root meristem of *teb pol2a* double mutants is severely compromised

A-F: Confocal images of root tips of 8-day-old plants stained with propidium iodide. A: WT (Col0), B: *teb2*, C: *teb5*, D: *pol2a-4*, E: *pol2a teb2* F: *pol2a teb5*. The meristem of *teb* mutants showed abnormal organization and cell death. This defect was exacerbated in *pol2a teb* double mutants with root hair differentiating close to the root tip and meristem organization being dramatically altered. Red arrow indicates the limit of the root apical meristem. Bar = 50 μ m for all panels.

G: Meristem length was measured in all mutant combinations. Values are from at least 10 roots and are representative of two independent experiments. Different letters indicate statistically relevant differences (ANOVA and Tukey test $p < 0.01$).

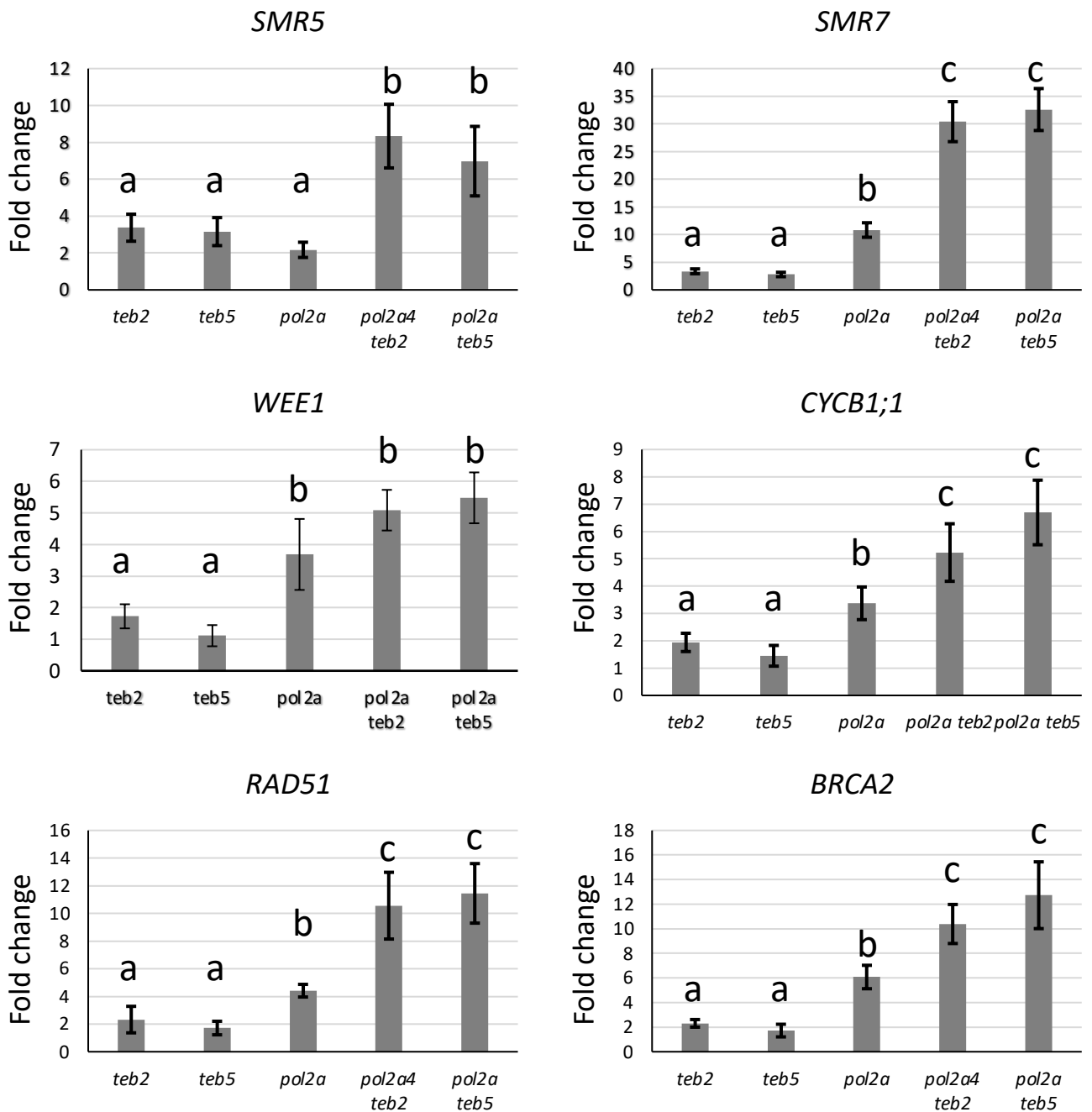


Figure 5. DDR genes are hyper-induced in *teb pol2a* double mutants

Total RNA was extracted from twelve-day-old plantlets. Expression of selected genes was assessed by real-time qPCR and normalized to actin. We monitored the expressions of genes involved in cell-cycle arrest (*SMR5*, *SMR7* and *WEE1*), DNA repair (*RAD51* and *BRCA2*) and both (*CYCB1;1*). Values are Fold change compared to the wild-type Col-0. Graphs represent average of 3 technical replicates +/- standard deviation and are representative of 3 independent biological replicates. Different letters above bars denote statistically relevant differences (ANOVA followed by Tukey test, performed on raw data before normalization, $p < 0.01$).

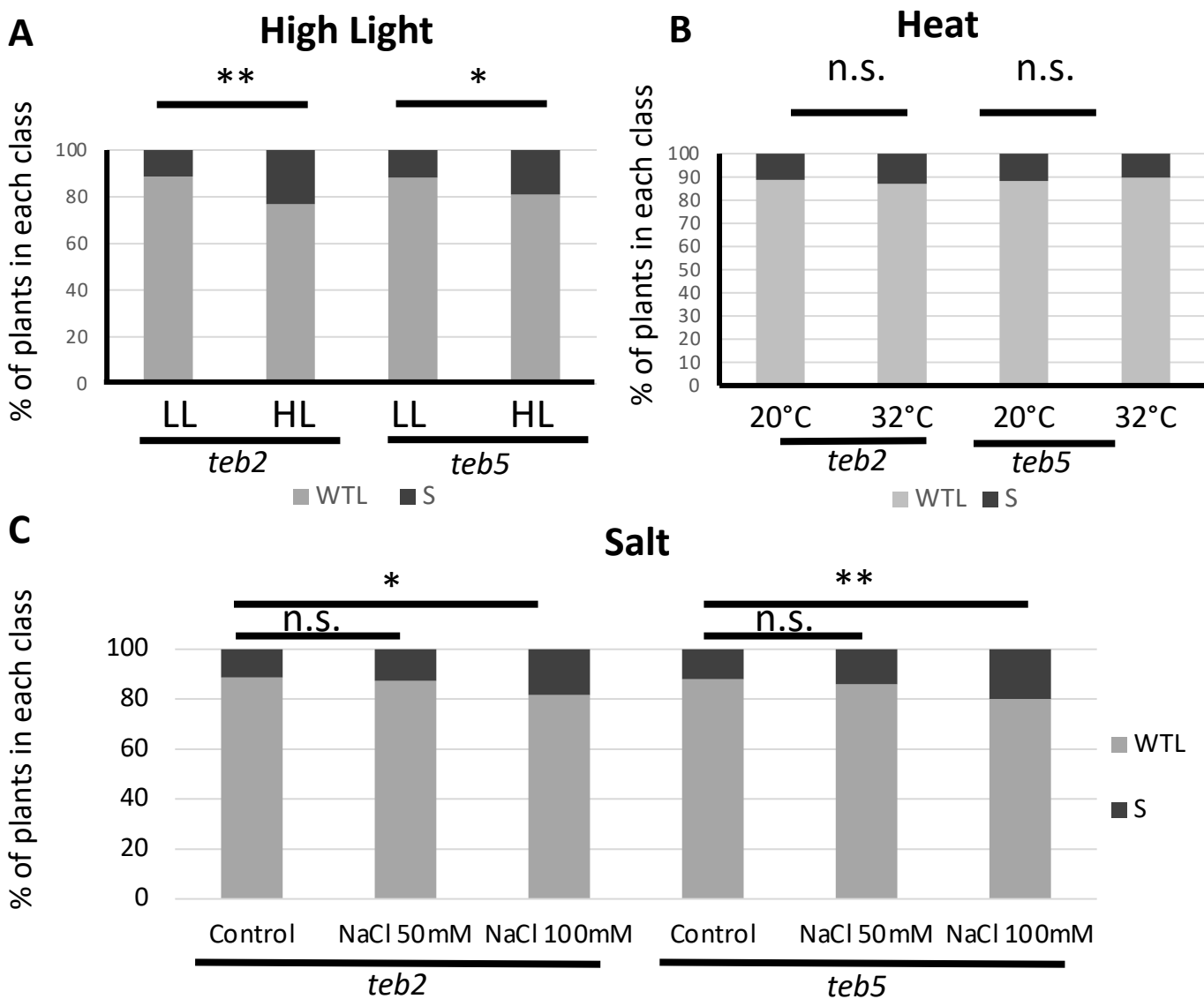


Figure 6: Some abiotic stresses aggravate the developmental defects of *teb* mutants.

A: Distribution of *teb* mutants between the different classes in plants grown in low light (LL, $160\mu\text{mol} \times \text{m}^{-2} \times \text{s}^{-1}$) or high light (HL, $350\mu\text{mol} \times \text{m}^{-2} \times \text{s}^{-1}$).

B: Distribution of *teb* mutants between the different classes in plants grown at standard temperature (20°C) or under heat stress (32°C). Plants were germinated *in vitro* and transferred to soil after 10 days. After 3 days of growth under control conditions at $160\mu\text{mol} \times \text{m}^{-2} \times \text{s}^{-1}$ plants were kept under the same conditions or transferred to 32°C under the same light intensity.

C: Distribution of *teb* mutants between the different classes in plants watered with or without salt to the indicated concentration. Plants were germinated *in vitro* and transferred to soil after 10 days. After 3 days of growth under control conditions ($160\mu\text{mol} \times \text{m}^{-2} \times \text{s}^{-1}$, 20°C , salt-treated plants were watered with a solution containing NaCl (50 mM), for the 100 mM treatment, salt concentration was increased to 100 mM after 2 days.

For all panels, n.s. indicates non-significant differences and asterisks denote statistically relevant differences between distributions (χ^2 -test, $p < 0.01$). Blind scoring was performed on wild-type and *teb* mutants in all growth conditions, the proportion of severe phenotypes observed in wild-type plants was below 2%.

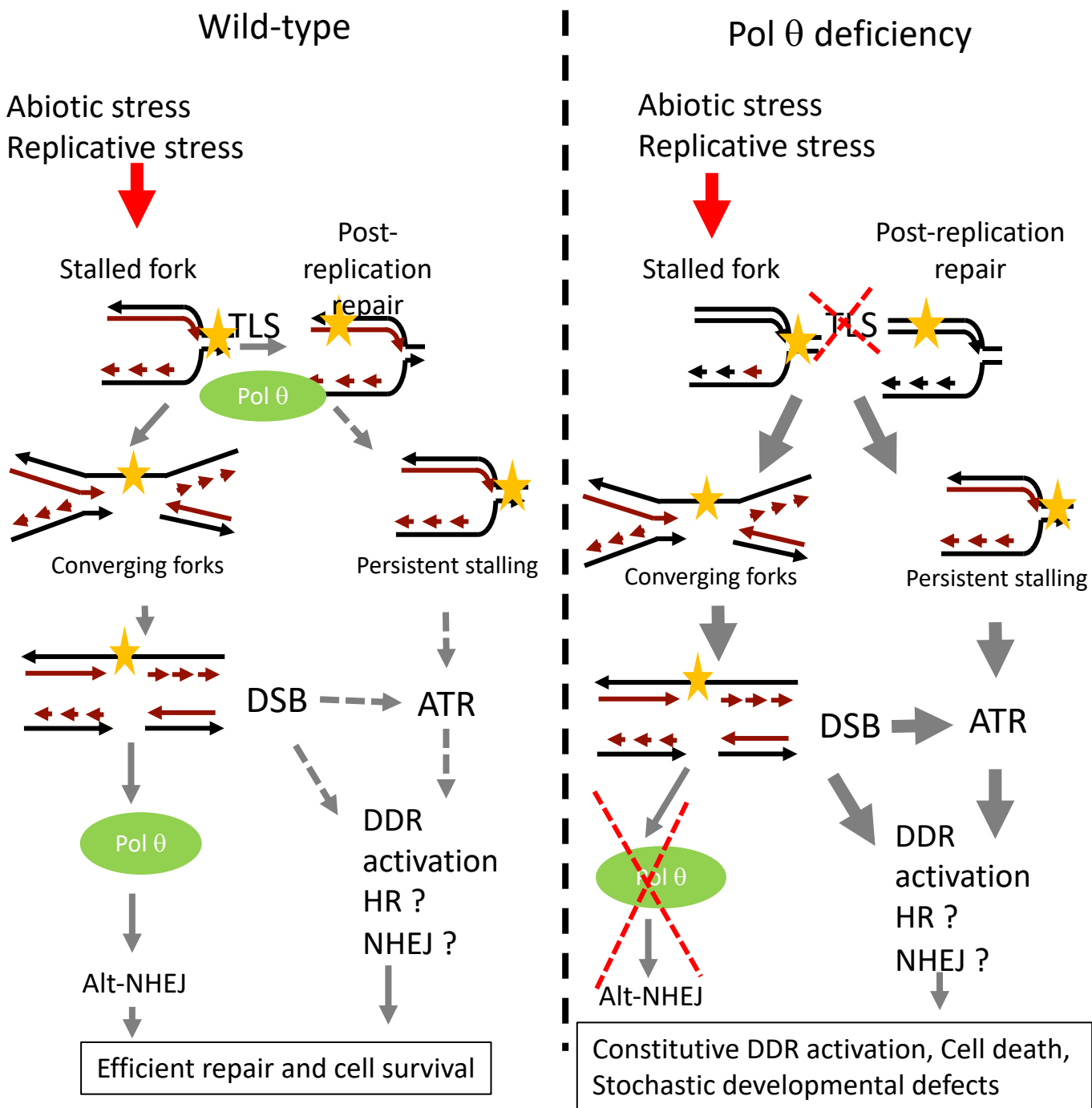


Figure 7: Model for the role of Pol θ during replicative stress response

A: In the wild-type, replication blocking lesions induce fork stalling. Pol θ can allow TLS through some lesions such as pyrimidine dimers. If efficient lesion bypass cannot be achieved, replisome disassembly and persistent fork stalling activates the DDR through ATR signalling, and DNA synthesis from a converging fork can lead to the formation of a double-ended DSB. Pol θ contributes to the repair of these lesions through Alt-NHEJ but other pathways such as HR or NHEJ likely contribute to DSB repair.

B: In the absence of Pol θ, TLS through some lesions is compromised, leading to an increased frequency of fork collapse and persistent stalling. Furthermore, Alt-NHEJ is also compromised, leading to an increased frequency of failed repair, constitutive activation of the DDR through ATR signalling, cell death and stochastic developmental defects. Abiotic stress and replicative stress can modify this equilibrium by enhancing the accumulation of more replication-blocking lesions, leading to an increased frequency of developmental defects in Pol θ deficient lines.

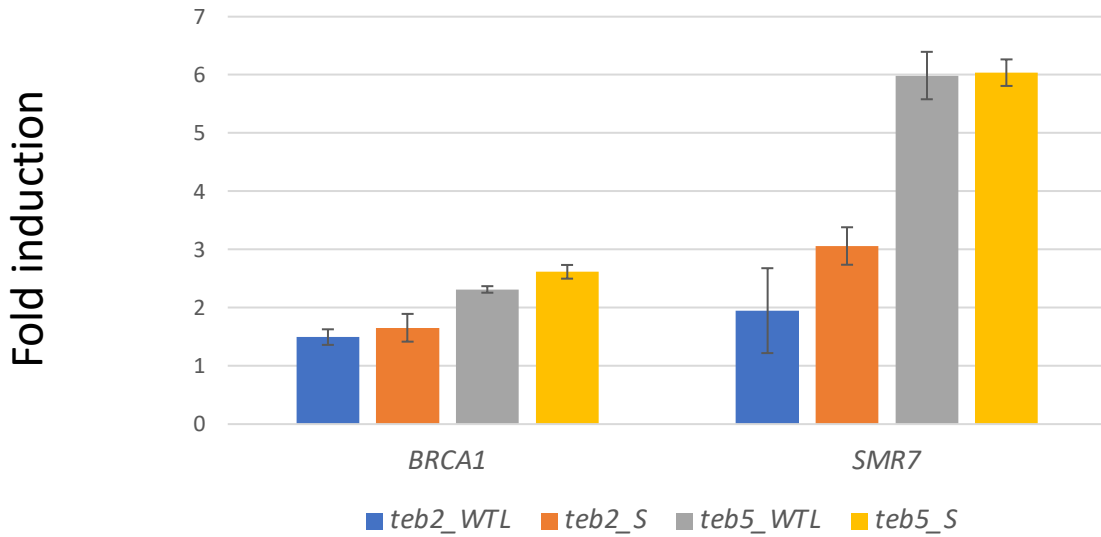


Figure S1. Levels of DDR genes induction do not correlate with the severity of *teb* mutants' phenotype. Expression of the DDR marker genes *BRCA1* and *SMR7* was monitored by qRT-PCR in rosette leaves of WTL and *S tebichi* mutants. Expression was normalized to that of *ACTIN*. Data are average +/- standard deviation of 3 technical replicates and representative of two independent experiments.

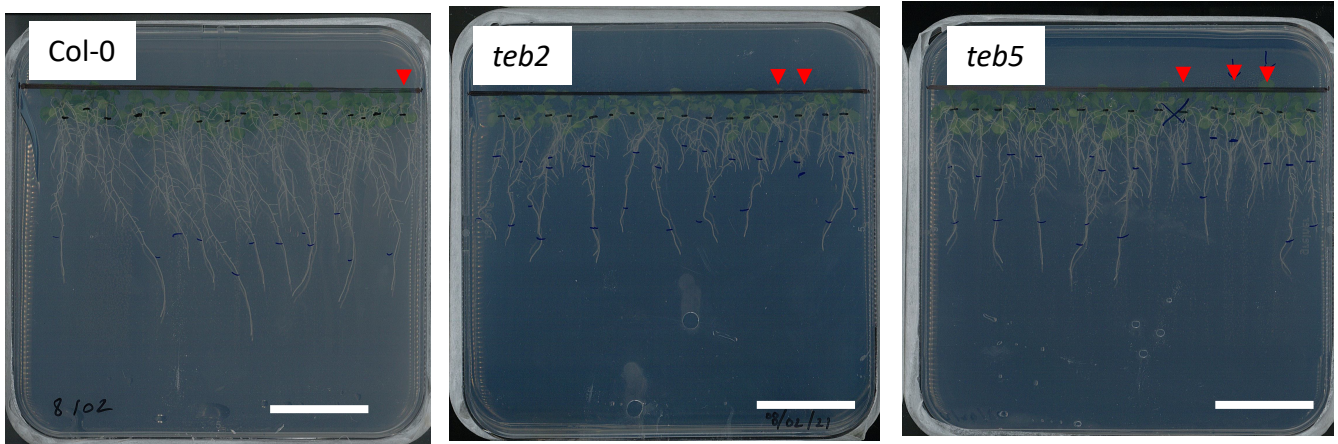


Figure S2. Root growth defects show some heterogeneity in *teb* mutants

Plantlets of the wild-type (Col-0) and *teb2* and *teb5* mutants were grown in vitro for 5 days, and aligned on half strength MS plates to be grown vertically. After 2 weeks, root growth of some plants appeared completely arrested in all genotypes (red arrowheads). The proportion of plants with arrested root growth was significantly higher in *teb* mutants (16% in *teb2* and 17% in *teb5*) than in the wild-type (7%), $n = 75$ for all genotypes, χ^2 p-value < 0.001. Bar = 2cm for all pictures.

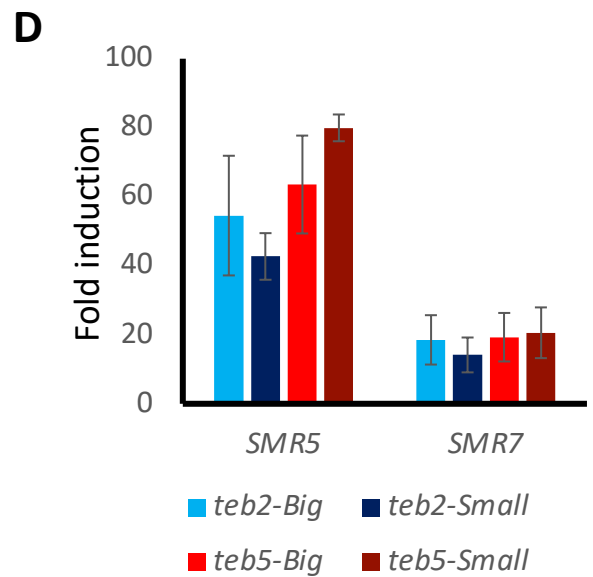
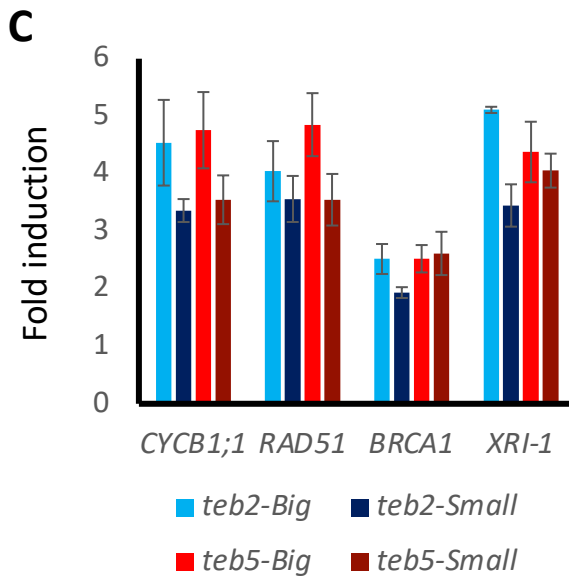
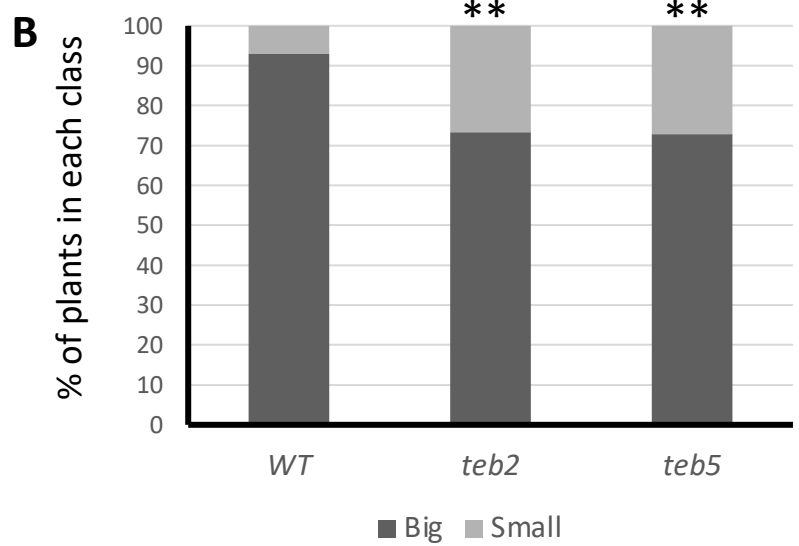
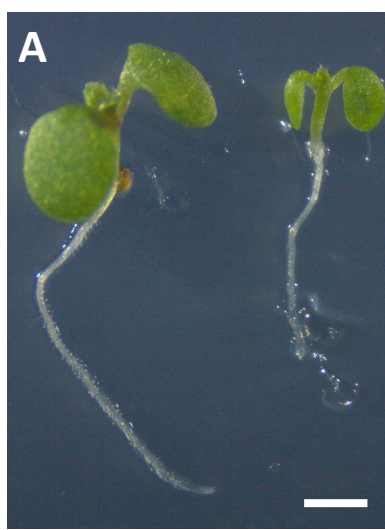


Figure S3. Heterogeneous phenotypes of *teb* mutant plantlets do not correlate with different levels of DDR genes activation

A: Representative picture of “big” and “small” plantlets observed among the *teb* mutants 10 days after germination, Bar = 500µm. B: Percentage of “big” and “small” plants among wild-type (WT) and *teb2* and *teb5* mutants (n>150 for all genotypes). ** denote statistically relevant differences χ^2 test p-value < 0.01. Data are representative for 3 independent experiments. C-D: qPCR analysis of DDR maker genes expression in small and big *teb* mutant plantlets. Expression levels were normalized using ACTIN as a reference gene, and results are expressed as fold-changed compared to the wild-type (Col-0). Data are average +/- standard deviation obtained from 3 technical replicates and are representative of 2 independent experiments.

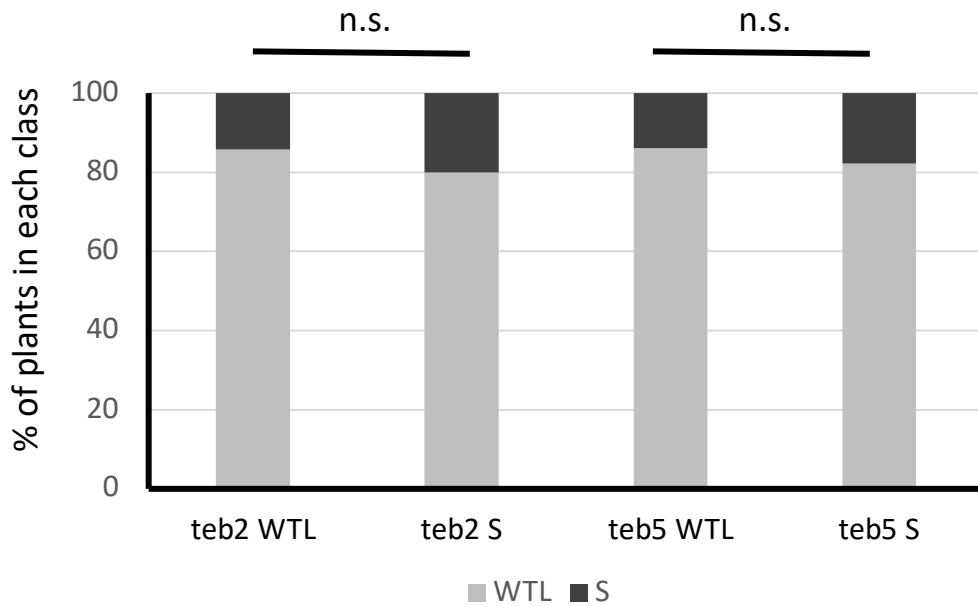


Figure S4. The *teb* phenotype does not aggravate over generations

Seeds from *teb* mutants with WTL and S phenotype were harvested and the distribution of individuals in each phenotypic category was estimated at the next generation. All three phenotypic classes were found in the progeny of each type of mutant, and no difference was observed in the distribution among the different classes between the three types of plants (χ^2 -test $p > 0.05$).

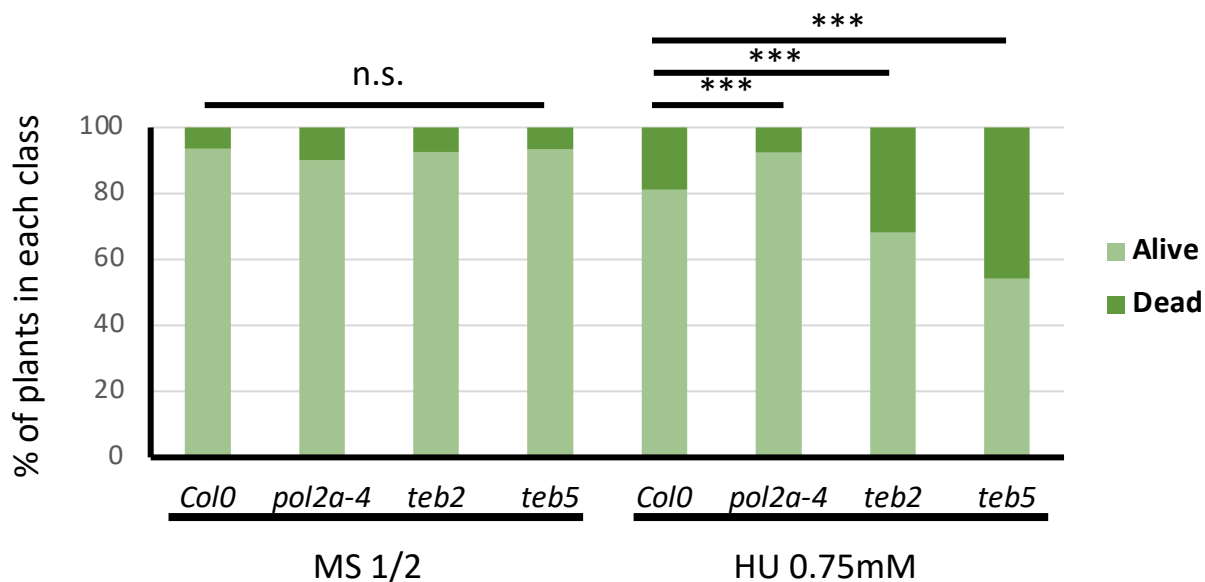


Figure S5. *teb* mutants are hypersensitive to replicative stress

Wild-type (Col0) and *teb* mutants (*teb2* and *teb5*) were germinated on MS supplemented or not with HU to a final concentration of 0.75mM. After 10 days, the survival rate was measured (n>100). While the survival rate on control medium was similar for all genotypes, *teb* mutants showed a higher proportion of dead plantlets on HU supplemented medium (χ^2 -test, p<0.001). The *pol2a-4* that was shown to be tolerant to HU (Pedroza-Garcia et al, 2017) was used as a control.

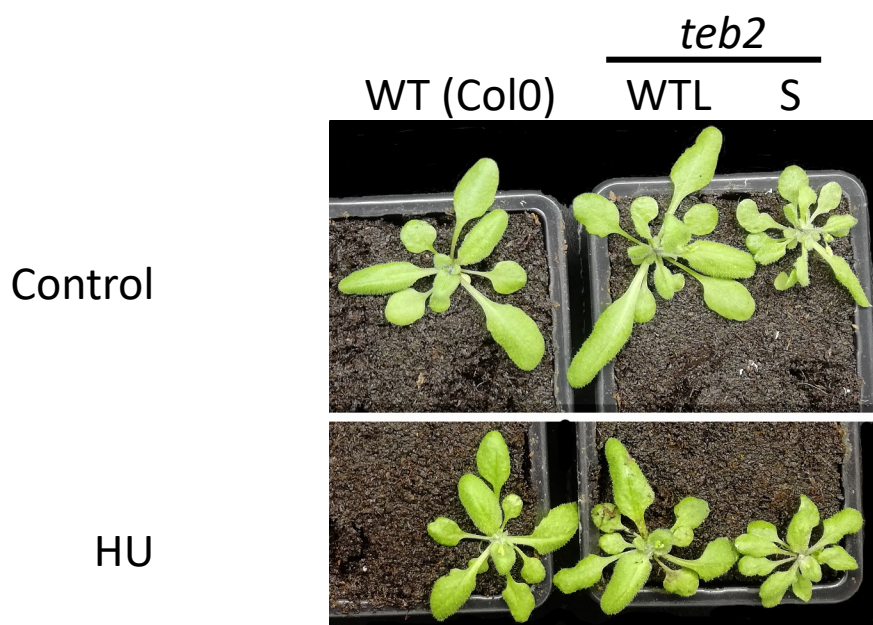


Figure S6. Representative phenotypes of wild-type (Col0) and *teb* mutants exposed to HU before transfer to the green house

Plants were grown for 10 days on half strength MS with or without HU (0.75mM). Surviving plants were transferred to the green house and grown for 3 weeks. Wild-type plants pre-treated with HU were slightly smaller than plants grown on MS alone. However, the characteristic *teb*-like phenotype was observed only amongst *teb* mutants.

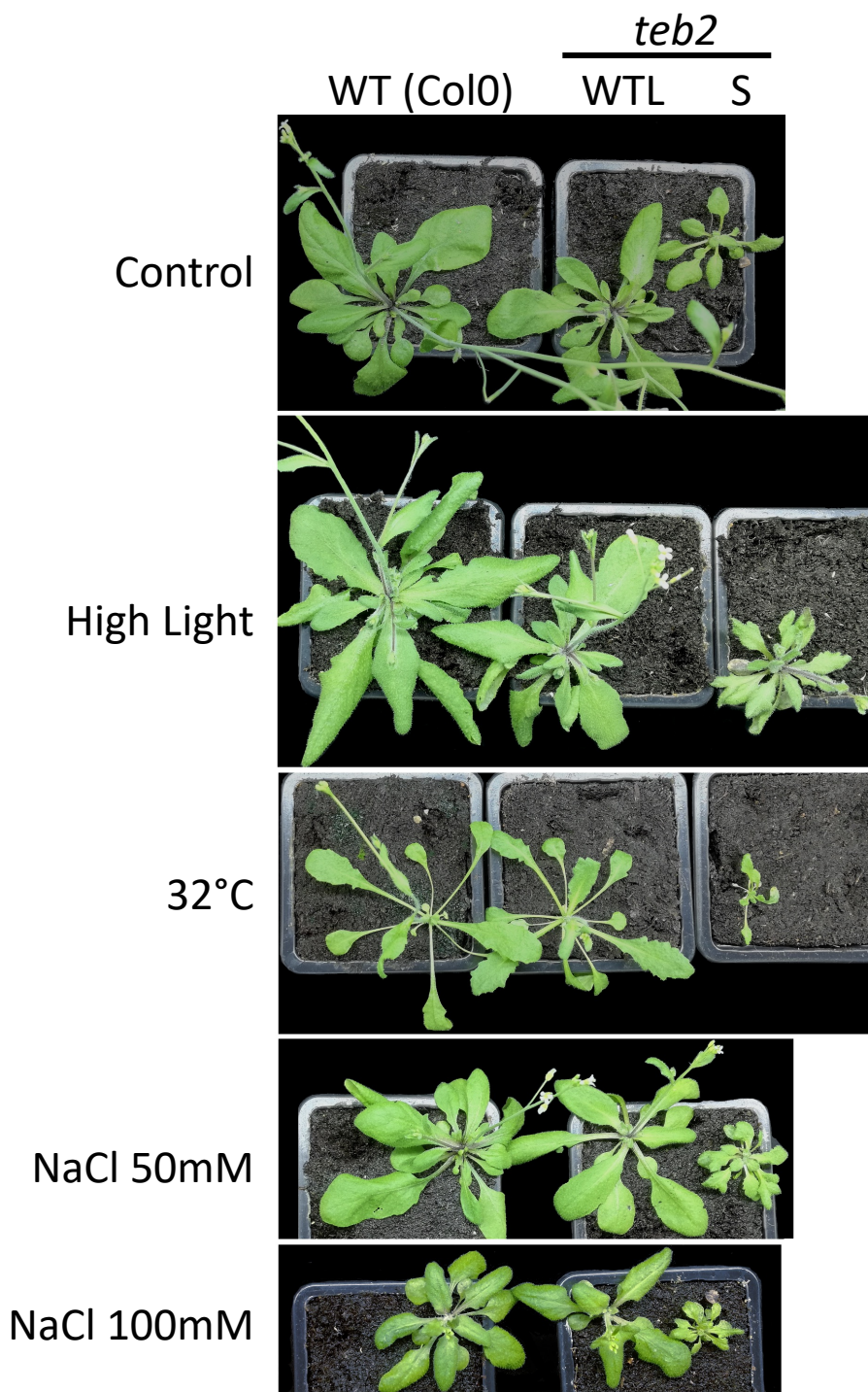


Figure S7. Representative phenotypes of wild-type (Col0) and *teb* mutants grown under different conditions.

Plants were grown for 1 month under the indicated conditions (see methods for details). Some of these growth conditions significantly altered the phenotype of wild-type plants: plants grown under high light were slightly larger with rolled leaves, plants grown at 32°C showed typical phenotype of plants acclimated to heat including elongated petiole and small leaf blade, while plants grown in the presence of salt showed reduced growth. The same modifications were observed in *teb* WTL plants. Moreover, none of these conditions induced the typical *teb*-like phenotype in wild-type plants.

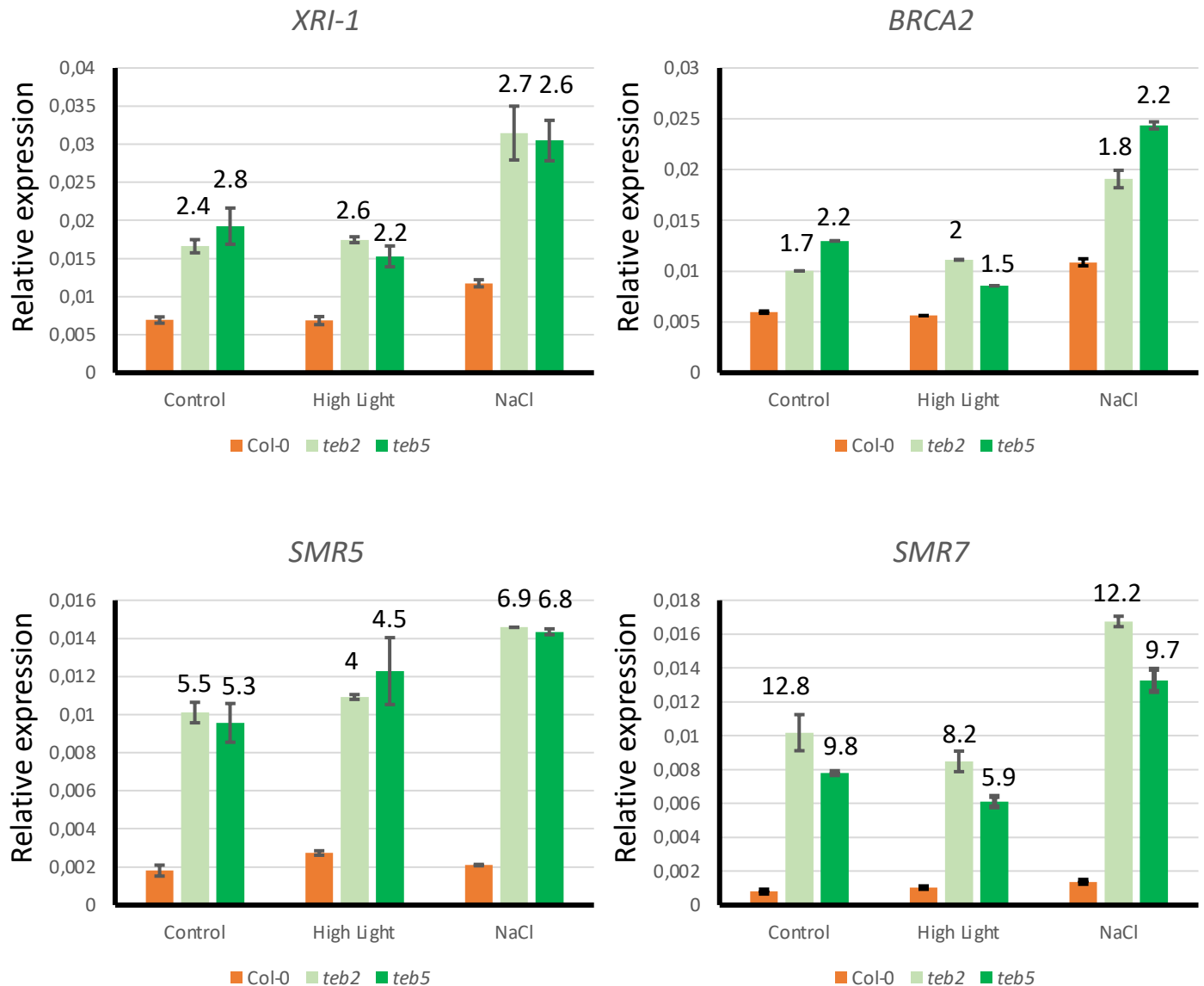


Figure S8. Salt treatment, but not increasing light intensity activates DDR gene expression in both wild-type and *teb* mutants.

Expression of DDR marker genes associated with DNA repair (*XRI-1* and *BRCA2*) or cell cycle arrest (*SMR5* and *SMR7*) was monitored by RT-qPCR in wild-type and *teb* mutants grown under standard conditions, germinated on NaCl supplemented medium (100mM) or exposed to high light. Data are average +/- S.D. obtained on 3 technical replicates and are representative of two independent experiments. They show relative expression of the selected genes compared to actin. Figures above bars represent the fold-induction compared to wild-type plants grown under the same conditions.